Pionic degrees of freedom and effects of nuclei near the point of pion condensation

I. N. Borzov, É. E. Sapershteĭn, S. V. Tolokonnikov, and S. A. Fayans

I. V. Kurchatov Institute of Atomic Energy, Moscow
Fiz. Elem. Chastits At. Yadra **12**, 848–904 (July–August 1981)

The state of the problem of π condensation in nuclei is reviewed. It is concluded from an analysis of various nuclear phenomena in which pionic degrees of freedom play an important part that there is probably no π condensate in nuclei but that they are close to the point of instability. The possible manifestations of this proximity in the inelastic scattering of nucleons and electrons by nuclei are discussed.

PACS numbers: 21.65. + f

INTRODUCTION

The problem of π condensation in nuclei has a history of almost a decade.[1-3] Initially, π condensation was regarded as an interesting but improbable conjecture, but it is now clear that although the phenomenon itself is not, apparently, present in real nuclei, its "rumblings" have an appreciable influence in many nuclear properties. In addition, it is now believed that a π condensate does exist in neutron stars, which leads to a number of very interesting astrophysical consequences.[4,5]

In the present review, we consider only the nuclear aspect of the π-condensate problem.

The first estimates of Migdal[1] showed that the situation in real nuclei is nearly critical, i.e., the parameters of the effective quasiparticle interaction in nuclei are close to the values at which the frequency of the "pionic mode" (spin–isospin zero sound) in nuclear matter vanishes. This occurs at a finite value $k = k_0 \sim p_F$ of the wave vector. It was immediately suspected that π condensation has already occurred in nuclei, and that they possess a periodic spin–isospin structure with characteristic period of order $1/k_0$. Further investigations showed that this is probably not the case. We shall discuss this question in detail and mention here the absence of appreciable single-nucleon widths of the levels of π atoms,[6] contradicting the theoretical prediction should a π condensate exist,[7] and also the absence of doublets of levels with opposite parity[3,8] in the spectra of the low-lying states of heavy nuclei. On the other hand, it is possible that nuclei are close to the point of the π-condensate instability. Such a possibility is interesting not only in that it leads to a number of important consequences for nuclear physics at low and medium energies but also in making probable the existence of anomalous superdense nuclei in which π condensation has occurred. The resulting energy gain in this case fully or partly offsets the contribution of nuclear compressibility. The conjecture of the existence of superdense nuclei of this kind[1,9] appears more realistic than the analogous conjecture by Lee and Wick[10] of anomalous nuclei produced by rearrangement of the so-called σ field.

Hitherto, all arguments in favor of relative proximity of nuclei to the point of π condensation have been quantitative and based on analysis of the spectra of states of anomalous parity ($0^-, 1^+, 2^-, \ldots$) and the M1 characteristics of nuclei.[11-13] It is therefore natural to look for phenomena in which the proximity of π condensation leads to qualitative effects. These are known in the literature as precritical effects, and the main aim of the present review is to analyze such phenomena in nuclei. However, we shall not consider the many problems associated with the interaction of slow pions with nuclei, which could be the subject of a separate review.

In Ref. 14, one phenomenon of the kind in which we are interested was pointed out—inelastic scattering of nucleons by nuclei with the excitation of states of anomalous parity. It was shown that if nuclei are near π condensation the differential reaction cross section at angles corresponding to momentum transfers $k \sim p_F$ will contain a characteristic maximum, whose height and width are determined by the proximity to the point of π condensation.

The possibility of precritical phenomena was also discussed by Gyulassy and Greiner[15] in connection with the collision of relativistic heavy ions and, in a larger aspect, by Ericson and Delorme,[16] in which precritical phenomena in nuclei were considered as "critical opalescence" (by analogy with phenomena in classical liquids near the critical temperature). In collaboration with Figureau and Giraud, the same authors[17] considered precritical effects in the inelastic magnetic scattering of electrons by light nuclei with the excitation of anomalous-parity states. Precritical effects in the inelastic scattering of protons by nuclei have also been discussed by Toki and Weise.[18]

The review is arranged as follows. In Sec. 1 we formulate the equations of the theory of finite Fermi systems with separated one-pion exchange, and in Sec. 2 we consider the conditions of stability with respect to π condensation in finite nuclei. In Sec. 3, we discuss the arguments which indicate that there is no π condensate in nuclei. Section 4 analyzes the spectroscopic characteristics of nuclei [the spectra, magnetic moments, and $B(M1)$] with the aim of extracting the interaction parameters that govern the phenomenon of π condensation. The set of constants found in the analysis indicates that nuclei are near the point of π condensation. In Sec. 5, we discuss the physical picture which arises in nuclei near π condensation. Sections 6 and 7 occupy a central position in the review. We here discuss precritical effects in the scattering of nucleons

 0090-4759/81/040338-24$02.80

(Sec. 6) and electrons (Sec. 7). Section 8 contains the main conclusions.

We thank S. T. Belyaev, V. M. Galitskiĭ, A. B. Migdal, I. N. Mishustin, V. M. Timofeev, M. A. Troitskiĭ, and V. A. Khodel' for very helpful discussion of the questions considered in the review.

1. SEPARATION OF ONE-PION EXCHANGE IN THE EQUATIONS FOR FINITE FERMI SYSTEMS

The basic equations in the theory of finite Fermi systems are the equation for the two-particle scattering amplitude

$$\Gamma = \mathcal{F} + \mathcal{F} A \Gamma \tag{1}$$

and the equation for the effective field:

$$V = e_q V_0 + \mathcal{F} A V. \tag{2}$$

Here, A is the particle–hole propagator, an integral over the energy of the product of two quasiparticle Green's functions,

$$A(\mathbf{r}, \mathbf{r}'; \omega) = \int \frac{d\varepsilon}{2\pi i} G\left(\mathbf{r}, \mathbf{r}'; \varepsilon - \frac{\omega}{2}\right) G\left(\mathbf{r}', \mathbf{r}; \varepsilon + \frac{\omega}{2}\right), \tag{3}$$

and $\mathcal{F}$ is the irreducible amplitude of the quasiparticle interaction, which does not contain diagrams with two lines in the annihilation channel. It differs from the vacuum nucleon–nucleon amplitude by having more complicated diagrams, these leading moreover to the appearance in (2) of the local charge e_q of the quasiparticles relative to the external field V_0. Initially, the theory of finite Fermi systems was intended to describe phenomena in which small momentum transfers k ($\ll p_F$) play the dominant part. In this case, $\mathcal{F}$ in Eqs. (1) and (2) is the amplitude of quasiparticle scattering at the Fermi surface through zero angle. However, it soon became clear that there are few such phenomena in nuclei. Large momenta are important, although for entirely different reasons, in the description of low-lying excitations for both electric[19,20] and magnetic[11,21] type. In this case, it is necessary to introduce a dependence of $\mathcal{F}$ on k. In the first case, this is usually done phenomenologically[20]; in the second, one separates from $\mathcal{F}$ the amplitude $\mathcal{F}_\pi$ of one-pion exchange in the annihilation channel.[3,11]

This separation is justified by the circumstance that one-pion exchange induces the nuclear forces with the longest range; for the characteristic momentum over which $\mathcal{F}_\pi(k)$ varies is $k \sim m_\pi \sim p_F/2$ (here and in what follows, $\hbar = c = 1$), whereas the characteristic momentum over which $\mathcal{F}_0 = \mathcal{F} - \mathcal{F}_\pi$ varies is of the order of the reciprocal core radius r_c ($k \sim 1/r_c > 2p_F$). Therefore, in a first approximation the dependence of $\mathcal{F}_0$ on k can be ignored. Note that $\mathcal{F}_0$ also includes the amplitude of one-pion exchange in the scattering channel, since it does not have a strong dependence on the momentum transfer k.[3]

Thus, we represent $\mathcal{F}$ in the form

$$\mathcal{F} = \mathcal{F}_0 + \mathcal{F}_\pi(\mathbf{k}), \tag{4}$$

where $\mathcal{F}_0$ does not depend on $\mathbf{k}$, and

$$\mathcal{F}_\pi(\mathbf{k}) = C_0 t(k^2)(\sigma_1 \mathbf{k})(\sigma_2 \mathbf{k}) \tau_1 \tau_2. \tag{5}$$

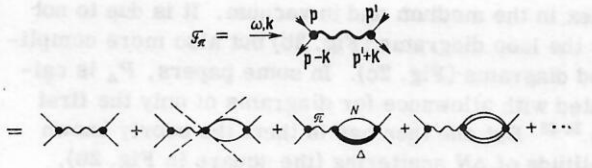

FIG. 1. The amplitude $\mathcal{F}_\pi$ of one-pion exchange in the annihilation channel in a nuclear medium. The broken lines exclude the diagram which, by definition, does not occur in $\mathcal{F}$.

Here, $C_0 = (dn/d\varepsilon_F)^{-1} = \pi^2/p_F m^* = 360$ MeV · F^3. Since we shall be interested in only low frequencies $\omega \ll \varepsilon_F < m_\pi$, we can ignore the ω dependence in $\mathcal{F}_\pi$, as in $\mathcal{F}_0$, and set $\omega = 0$ in both. Because of the effects of the medium, $t(k^2)$ in (5) differs from the vacuum function

$$t_0(k^2) = C_0^{-1} (g_{\pi N}/2m)^2 \mathcal{D}_0(\omega = 0, k) = -1.15/(k^2 + m_\pi^2), \tag{6}$$

where $\mathcal{D}_0(\omega, k) = \omega^2 - k^2 - m_\pi^2$ is the propagator of the free pion.

Let us analyze the diagrams which cause t to differ from t_0. The amplitude $\mathcal{F}_\pi$ corresponds to the diagrams in Fig. 1, in which the thick wavy line represents the propagator $\mathcal{D}$ of the pion in the nuclear medium, this being irreducible in the same sense as $\mathcal{F}$. It is related to $\mathcal{D}_0$ (the thin wavy line) by the usual Dyson equation:

$$\mathcal{D} = \mathcal{D}_0 - \mathcal{D}_0 P \mathcal{D}. \tag{7}$$

As is clear from the foregoing, the polarization operator P in this equation is not complete, since it does not contain the particle–hole term A. The most important term $P(P_\Delta)$ is associated with virtual production of the Δ isobar (Fig. 2). In Ref. 3, there is a detailed investigation of the various terms in P, including the contribution of s-wave scattering and the contributions of the more distant p-wave resonances. Here, following Refs. 1 and 11, we use for P an expression in which the contribution of the s-wave scattering is ignored; it is important for a neutron medium,[3] but in the case of symmetric nuclear matter is small. The influence of the distant resonances is taken into account phenomenologically by the introduction of a dependence of the $\pi N \Delta$ form factor on k by extrapolating the experimental data[22] to the region $\omega \sim 0, k \sim p_F$:

$$P = -\frac{0.9(1-\alpha)k^2}{1 + 0.23k^2/m_\pi^2} \frac{n(r)}{n(0)}. \tag{8}$$

Here, $n(r)$ is the density of nuclear matter at the point r, and $n_0 = 0.147$ F^{-3} is the density of normal nuclear matter.[23] The factor $1 - \alpha$ in (8) is introduced to take into account the possible difference between the $\pi N \Delta$

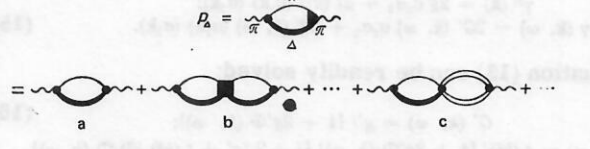

FIG. 2. The polarization operator P_Δ. The black point in the upper diagram is the vacuum $\pi N \Delta$ interaction vertex, and the black triangle is the corresponding vertex in a medium; the black square in diagram b is the amplitude of $N\Delta$ scattering.

vertex in the medium and in vacuum. It is due to not only the loop diagrams (Fig. 2b) but also more complicated diagrams (Fig. 2c). In some papers, P_Δ is calculated with allowance for diagrams of only the first type.[24,25] But one then has in them the poorly known amplitude of ΔN scattering (the square in Fig. 2b), about which rather arbitrary assumptions are made. We prefer to regard α in (8) as a phenomenological parameter. In Ref. 3, the estimate $0.3 > \alpha > -0.2$ is obtained for α. The expression for P in Ref. 3 with allowance for s-wave scattering and the distant p-wave resonances differs little from (8) at $k \sim p_F$.

The function $t(k^2)$ in (5) is obtained from (6) by replacing $\mathscr{D}_0$ by $\mathscr{D}$ and multiplying by the factor $(e_q^\pi)^2$, and each vertex in Fig. 1 includes the local charge e_q^π with respect to the field $(\sigma \cdot k)\tau_\alpha$. The characteristic scale of the momenta that determine the dependence of e_q^π on k is the same as in the case of $\mathscr{F}_0$, and for the same reason this dependence can be ignored, so that one takes[11]

$$e_q^\pi(k) = e_q^\pi(k=0) = 1 - 2\zeta_s, \tag{9}$$

where ζ_s is the constant which occurs in the local charge for the field $\sigma_\alpha\tau_\beta$ (Ref. 26): $e_q[\sigma_\alpha\tau_\beta] = 1 - 2\zeta_s$. It is known from analysis of the magnetic moments that $0 \leq \zeta_s \leq 0.1$. As a result,

$$\mathscr{F}_\pi = -1.15(1-2\zeta_s)^2 \frac{(\sigma_1 k)(\sigma_2 k)\tau_1\tau_2}{m_\pi^2 + k^2 + P(k)}, \tag{10}$$

where $P(k)$ is given by Eq. (8). In the expression for $\mathscr{F}_0$, we have restricted ourselves to the contribution of the zeroth harmonics:

$$\mathscr{F}_0 = C_0[f_0 + f_0'\tau_1\tau_2 + (g_0 + g_0'\tau_1\tau_2)\sigma_1\sigma_2]. \tag{11}$$

2. π-CONDENSATE INSTABILITY IN NUCLEI

Symmetric nuclear matter. The existence in the spin–isospin part of the amplitude $\mathscr{F}$ of a repulsive ($\sim g' > 0$) a and an attractive ($\mathscr{F}_\pi$) term makes it possible for complex frequencies to arise in Eqs. (1) and (2), which means that the system is unstable. We consider first the conditions for the occurrence of such instability in infinite nuclear matter, for which the particle–hole propagator is

$$A(k, \omega) = -C_0^{-1}\Phi(k, \omega), \tag{12}$$

where $\Phi(k,\omega)$ is the well-known Linhard function.[27] Going over in (1) to the dimensionless amplitudes $\gamma^\omega = C_0^{-1}\mathscr{F}$ and $\gamma = C_0^{-1}\Gamma$, we obtain in the spin–isospin channel

$$\gamma(\mathbf{k}, \omega) = \gamma^\omega(\mathbf{k}) - \gamma^\omega(\mathbf{k})\Phi(k, \omega)\gamma(\mathbf{k}, \omega), \tag{13}$$

where

$$\gamma^\omega(\mathbf{k}) = 2g'\sigma_1\sigma_2 + 2t(k^2)(\sigma_1\mathbf{k})(\sigma_2\mathbf{k}); \tag{14}$$

$$\gamma(\mathbf{k}, \omega) = 2G'(k, \omega)\sigma_1\sigma_2 + 2T(k, \omega)(\sigma_1\mathbf{k})(\sigma_2\mathbf{k}). \tag{15}$$

Equation (13) can be readily solved:

$$G'(k, \omega) = g'/[1 + 2g'\Phi(k, \omega)]; \tag{16}$$

$$T(k, \omega) = t(k^2)/[1 + 2g'\Phi(k, \omega)][1 + 2(g' + t(k^2)k^2)\Phi(k, \omega)]. \tag{17}$$

Equation (2) for the effective field V in nuclear matter in the presence of an external field $(V_0)_\alpha^\beta = v_0(k) \times \sigma_\alpha\tau_\beta \exp(i\mathbf{kr})$ can be solved similarly:

$$V_\alpha^\beta(k, \omega) = [V_1(k, \omega)\sigma_\alpha + V_2(k, \omega)(\sigma\mathbf{k})k_\alpha/k^2]\tau_\beta, \tag{18}$$

where

$$V_1(k, \omega) = v_0(k)/[1 + 2g'\Phi(k, \omega)], \tag{19}$$

and

$$V_2(k, \omega) = -v_0(k)\,2t(k^2)k^2\Phi(k, \omega)/[1 + 2g'\Phi(k, \omega)] \times [1 + 2(g' + t(k^2)k^2)\Phi(k, \omega)]. \tag{20}$$

It can be seen from (16)–(20) that the spectrum of spin–isospin excitations is determined by the dispersion relations

$$1 + 2g'\Phi(k, \omega) = 0; \tag{21}$$

$$1 + 2(g' + t(k^2)k^2)\Phi(k, \omega) = 0. \tag{22}$$

Since the constant g' is positive, $g' > 0$, the first of these equations has a solution only for $\omega > kv_F$ ($v_F = p_F/m^*$) and never leads to instability.[3] In the second equation solutions with negative ω^2, indicating instability of the system, are possible in the case of certain relationships between g' and the parameters ζ_s and α in $t(k^2)$. This instability is called the π-condensate instability.

Equation (22) was considered in detail in Ref. 3. In fact, a more general dispersion relation was studied with allowance for the ω^2 dependence of P and the pion propagator. This general relation gives three branches of solutions, of which we consider only the lowest, which leads to π condensation, for which these dependences are not important. At small k, the solution of (22) is virtually the same as the solution of (21). With increasing k, it approaches the straight line $\omega = kv_F$ (Fig. 3), and then the stationary solution of (22) vanishes (because of the imaginary part in Φ for $\omega < kv_F$). For $\omega^2 < 0$ and $k \sim p_F$, a solution which increases with the time and corresponds to the π-condensate instability can be obtained. In finite nuclei, the imaginary part of Φ is nonzero only for $\omega > \Delta\varepsilon_\lambda$, where $\Delta\varepsilon_\lambda$ is the first particle–hole difference. Having in mind finite nuclei, we can represent Φ in the interval $0 < \omega < \Delta\varepsilon_\lambda$ in the form

$$\Phi(k, \omega) = \Phi_0(k) + \left(\frac{\partial\Phi}{\partial\omega^2}\right)_{\omega=0}\omega^2. \tag{23}$$

Then from (22) we obtain

$$\omega^2 = \tilde{\omega}^2(k)\left[-\frac{1 + 2g'\Phi_0}{2(\partial\Phi/\partial\omega^2)_{\omega=0}(m_\pi^2 + k^2 + P(k))(g' + t(k^2)k^2)}\right], \tag{24}$$

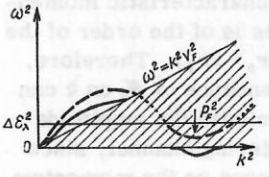

FIG. 3. Qualitative form of the dispersion law for spin–isospin sound in nuclear matter. The region in which there are no solutions with real ω because of Landau damping is hatched. The continuous curve corresponds to the case with π-condensate instability, and the broken curve to a situation close to instability (the lower part of the broken curve for $k^2 \sim p_F^2$ gives a nominal description of the excitation spectrum in a finite nucleus; $\Delta\varepsilon_\lambda$ is the first difference of the single-particle energies).

where

$$\tilde{\omega}^2(k) = m_\pi^2 + k^2 + P(k) - \frac{2.3(1-2\zeta_s)^2 k^2 \Phi_0}{1+2g'\Phi_0}. \quad (25)$$

The expression in the square brackets in (24) is positive and for $k \sim p_F$ has the estimate $\sim v_F^2 (\sim 1/10)$, and therefore

$$\omega^2 = \tilde{\omega}^2(k)\, v_F^2 \varphi(k), \quad (26)$$

where $\varphi(k)$ is a smooth function of k (of order unity). Thus, the vanishing of ω^2 is due to the vanishing of $\tilde{\omega}^2(k)$, i.e., the condition of π-condensate instability can be written in the form

$$\tilde{\omega}^2(k_0) = 0 \ (k_0 \sim p_F), \quad (27)$$

where $\tilde{\omega}^2(k)$ is determined by (25).

Figure 4 shows the dependences $g'_{cr}(\alpha)$ and $k_0(\alpha)$ for several values of ζ_s.

The π-condensate instability in finite nuclei. The instability of nuclear matter in the channel with pionic quantum numbers arises at wave vectors k of the order of the Fermi momentum p_F. Therefore, in sufficiently large nuclei with diameters much greater than p_F^{-1}, the picture of the instability must be approximately the same as in an infinite system, and the effects of the finite size must be important only near the boundary of the nucleus. Such a situation is considered in Ref. 28. However, it is still not clear whether real nuclei are sufficiently large for this situation to occur. In addition, in light nuclei the picture of the condensation may be different. All these questions were considered in Ref. 29 on the basis of an exact solution of the equations of the theory of finite Fermi systems in the coordinate representation for specific nuclei.

Expanding the effective field V with respect to spherical tensors and separating the angular variables (see Appendix 1), we obtain from (2) an equation that determines the eigenfrequencies ω_s for the different modes:

$$v_L^J(r;\omega_s) = \int_0^\infty r_1^2 dr_1 \int_0^\infty r_2^2 dr_2 \sum_{L'L''} \mathcal{F}_{LL'}^J(r, r_1) \times A_{L'L''}^J(r_1, r_2; \omega_s)\, v_{L''}^J(r_2; \omega_s). \quad (28)$$

Here, $v_L^J(r;\omega_s)$ is regarded as the amplitude for production of the state $|s\rangle$ with angular momentum J and parity $\pi = (-1)^L = (-1)^{J\pm1}$, so that the symmetry of the considered external field corresponds to states of anomalous parity $0^-, 1^+, 2^-, \ldots (V_0 \sim \sigma_\alpha \tau_\beta)$. For the amplitude v_L^J, we have the normalization condition[26]

$$\left(v \frac{dA}{d\omega} v\right)_{\omega=\omega_s} = -1, \quad (29)$$

where the brackets indicate integration over all the coordinates and summation over the spin–isospin indices [to simplify the expressions, these indices are omitted in (28)].

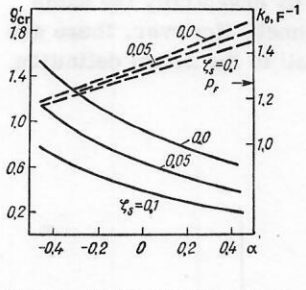

FIG. 4. Critical parameters of the amplitude $\mathcal{F}$ and the corresponding momenta k_0 (broken curves) at which the π-condensate instability arises in infinite nuclear matter. The parameters are found from the condition $\tilde{\omega}^2_{min}(k_0) = 0$ [$\tilde{\omega}^2_{min}$ is the minimum of the expression (25)] for $m_{\pi^0} = 0.684$ F^{-1}, $p_F = 1.27$ F^{-1}, and $n_0 = 0.138$ F^{-3}, which corresponds to $r_0 = 1.2$ F^{-1}.

We consider first the neutral channel ($V_0 \sim \sigma\tau_3$). In this case, instability corresponds to vanishing of the square of the eigenfrequency ω in Eq. (28). To elucidate the nature of the π-condensate instability, it is sufficient to find the critical values g'_{cr} as functions of the angular momentum J and the mass number A, i.e., to solve Eq. (28) with $\omega = 0$ for some fixed values of the other interaction parameters (g, α, and ζ_s). For simplicity, we shall in what follows discuss the case $g = 0.65$ and $\alpha = \zeta_s = 0$. For other sets, all the qualitative conclusions remain valid.[29] Calculations were made with Woods–Saxon potential taken from Ref. 30 for spherical nuclei in the range from ^{16}O to the hypothetical nucleus ^{298}114. The results are given in Table I. Analysis of them shows that g'_{cr} does not have any systematic dependence on A. Shell effects, particularly for magic nuclei, have a much stronger effect. It can be seen from Table I that in light and heavy nuclei these effects lead to two different situations.

Suppose that we could, by fiat, reduce the constant g' or, equivalently, increase the density n (the relative change δn in the density is related to the relative change in the constant g' by $\delta n/n \sim -\delta g'/g'$). Then in light nuclei instability of the 0^- mode occurs first. Estimates show[29] that the distance $\Delta g' \approx 0.05$ (for example, in ^{16}O and ^{40}Ca) to the nearest instability point of the 2^- mode is sufficiently great for the influence of the remaining modes on the 0^- instability to be ignored. Therefore, in the case of a phase transition of the second kind, or of the first but nearly one of the second, the structure of the condensate must correspond to the 0^- symmetry (alternation of layers with radial dependence $\sim j_1(k_0 r)$ and angular dependence $\sim Y_1(n)$; $k_0 \sim p_F$, and $j_1(x)$ is a spherical Bessel function).

TABLE I. Critical values g'_{cr} for different modes in nuclei (for $g = 0.65$, $\alpha = \zeta_s = 0$).

J^π	^{16}O	^{40}Ca	^{56}Ni	^{100}Sn *2	^{114}Sn	^{208}Pb	^{298}114 *2
0$^-$	0.87	0.99	0.98	0.94	0.95	0.97	0.96
1$^+$	0.76	0.83	0.87	0.88	0.91	0.89	0.91
2$^-$	0.82	0.92	0.95	0.94	0.96	0.96	0.95
3$^+$	0.50	0.79	0.89	0.93	0.92	0.90	0.93
4$^-$	—*	0.82	0.88	0.94	0.93	0.96	0.95
5$^+$	—	—	0.67	0.86	0.86	0.92	0.91
6$^-$	—	—	—	—	0.86	0.94	0.95
7$^+$	—	—	—	—	—	0.87	0.91
8$^-$	—	—	—	—	—	0.86	0.92

*It is meaningful to consider the instability for modes with angular momenta $J \lesssim A^{1/3}$.

2*These nuclei do not exist in stable form, but this is not important for the considered problem.

A different situation is realized in heavy nuclei, in which the instability points are divided into two groups—for the modes of negative and positive parity, respectively. Within each group, the instability points virtually coincide, but the distance between the groups is $\Delta g'_{cr} \approx 0.05-0.08$. The splitting is due to the circumstance that in nuclei the states in neighboring shells have, as a rule, opposite parity. This is a reflection of the quasioscillator form of the nuclear self-consistent potential well. In the limit $A \to \infty$, the splitting must vanish, states of both the same and the opposite parity being equally represented in a broad rectangular well. In real heavy nuclei, all the modes of negative parity condense first when the density increases smoothly. This means that for $g' \leqslant g'_{cr}$ we have the onset of spontaneous growth of fluctuations of the spin density with coordinate dependence $\sim \sin k_0 r$, and in the case of a phase transition of the second kind it is natural to assume that in such nuclei a condensate with the same spatial structure will arise. Note that such a situation is characteristic of magic nuclei, which are mainly represented in Table I. For the nonmagic nucleus ^{114}Sn, this effect is much weaker.

With regard to the regular dependence of the constant g'_{cr} on the mass number A, it is rather difficult to draw any definite conclusions on the basis of the calculations. If a comparison is made with the value of the critical constant in infinite nuclear matter ($g'_{cr\,\infty} = 0.91$), it can be seen that the phase transition to the π-condensate state in nuclei occurs at approximately the same value. However, a literal comparison is difficult, since there is a certain arbitrariness in the choice of the parameter used to make $dn/d\varepsilon_F$ dimensionless [the constant C_0 in the amplitude (5)]. Comparison of the critical constants in light nuclei, on the one hand, and heavy nuclei, on the other, with a view to establishing the nuclei in which π condensation occurs earlier is not very sensible, since the amplitude contains terms $\sim(N-Z)/A$,[31] whose contribution we have ignored. In principle, allowance for them can lead in heavy nuclei to corrections equivalent to a change in g'_{cr} by ≈ 0.05. There is some point in comparing the constants g'_{cr} for fixed J^π in nuclei with $N = Z$, i.e., ^{16}O, ^{40}Ca, ^{56}Ni, and ^{100}Sn (the last, it is true, does not exist, but this is not relevant to the considered question); it can be seen that with increasing A the constants g'_{cr} do indeed approach on the average the value in the infinite system. However, on the background of this approach fluctuations of shell nature are observed.

The critical conditions in finite nuclei were investigated from a somewhat different point of view by Meyer-ter-Vehn.[32] The calculations were also made in the coordinate representation, but the particle–hole propagator was found by summing over single-particle states in a large but nevertheless finite oscillator basis. It was not the critical values of the interaction parameters that were sought but rather the critical density n_{cr}; the variation of the density was achieved by varying the oscillator parameter. It was shown that stable results are obtained only when one takes into account not less than 16–18 principal oscillator shells;

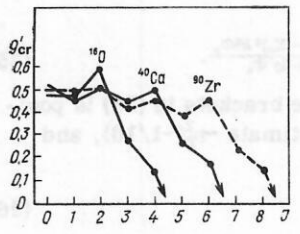

FIG. 5. Critical values $g'_{cr}(J)$ from Ref. 25.

this confirms once more the fact already noted in Ref. 29 that standard RPA calculations with truncated (two or three shells) basis cannot pretend to quantitative accuracy in the description of phenomena associated with the π-condensate instability. The shortcoming of an oscillator potential is that for heavy nuclei it differs strongly from the realistic potential. Nevertheless, the conclusions of Ref. 32 are qualitatively close to the results of the more realistic calculations of Ref. 29.

In Ref. 25, Toki and Weise also used an oscillator potential, but made the calculations in the momentum rather than the coordinate space. They calculated the so-called response function $R(k,k';\omega)$ up to a factor equal to the amplitude Γ [Eq. (1)]. Such an approach makes it possible to find not only the critical constants but also the critical momentum for given mode J^π, which permits a more direct comparison with the results of the calculations for infinite matter. Approximations of a numerical nature were made in the calculation of R, but qualitatively the results obtained in Ref. 25 agree with ours. It can be seen from Fig. 5 that, as in our calculations, g'_{cr} undergoes "even–odd jitter," remaining approximately constant up to $J \sim A^{1/3}$, after which it decreases rapidly. The appreciable differences between the g'_{cr} values in Table I and in Fig. 5 are due primarily to the different method used to take into account the contribution of the Δ isobar. Namely, Toki and Weise[25] introduce a δ-functional repulsion between the Δ isobar and the nucleon with the same constant g' as for nucleons. This corresponds to $\alpha \approx 0.5$ in the polarization operator (8), i.e., to a weakening of the contribution from the Δ isobar by approximately two times. It is this that causes the decrease in g'_{cr}.

The π-condensate instability in the charged channels ($V^\pm \sim \sigma\tau_\pm$) can be investigated by essentially the same scheme as in the neutral channel. However, there are some differences due above all to the actual definition

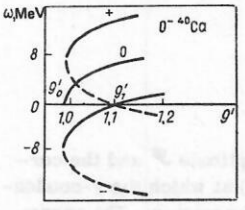

FIG. 6. Position of the first excited 0^- states in ^{40}Ca as a function of g' (the neutral and charged excitations are indicated by 0, +, and −, respectively).

of the stability conditions and the choice of the physical branches. We shall discuss these differences for the example of two nuclei: ^{40}Ca and ^{208}Pb.

It is simplest to illustrate the procedure for choosing the physical branches by examining graphs of the eigenfrequencies of Eq. (27) as functions of the constant g'. As an example, Fig. 6 shows such graphs for the 0^- mode in ^{40}Ca for $\alpha = \zeta_s = 0$ and $g = 0.65$ (for a neutral field; the constant g does not occur in the equations for charged fields). The indices + and – indicate the charged channels (respectively, for the field $V^+ \sim \sigma\tau_+$, which produces a $\bar{p}n$ (proton–neutron hole) pair, and the field $V^- \sim \sigma\tau_-$, which produces a $\bar{p}\bar{n}$ pair); the index 0 corresponds to the neutral channel (for the field $V^0 \sim \sigma\tau_0$, which produces $n\bar{n}$ and $p\bar{p}$ pairs). The effective field V^0 is a function of ω^2, and therefore the curve with index 0 is nearly a parabola at low frequencies. The curves with the indices + and – are shifted relative to it by the Coulomb energy (or rather, by $\Delta\mu = [E_B(^{41}\text{Sc}) - E_B(^{41}\text{Ca}) + E_B(^{39}\text{Ca}) - E_B(^{39}\text{K})]/2$, where $E_B(X)$ is the binding energy of nucleus X). These curves are the mirror images of each other with respect to the abscissa, which corresponds to the condition $V^+(\omega) = V^-(-\omega)$. Their shape almost exactly repeats the 0 curve, which is a consequence of isotopic invariance, which works rather well in the case of ^{40}Ca.

The prescription for choosing the physical branches in the language of the meson $\mathscr{D}$ function is considered in Ref. 3. In our case, this choice is much simpler, since in nuclei, in contrast to neutron matter, the branches that begin at small ω do not get entangled with the branches that begin at $\omega \sim m_\pi$. The prescription for the choice can be formulated as follows: With increasing repulsive interaction, i.e., with increasing constant g', the energy of the level must rise. The upper parts of the curves represented by the continuous lines meet this criterion. These are the physical branches. The "true" instability point for the charged channels, i.e., the point at which complex solutions arise (in the terminology of Ref. 3, the point of "pairing" instability), is the point $g' = g'_0$ (at it, the derivative $\partial\omega/\partial g'$ becomes infinite). This point virtually coincides with the instability point in the neutral channel. The point g'_1 at which the frequency $\omega^-(g')$ vanishes (apart from small corrections containing the electron mass, the neutron–proton mass difference, etc.), corresponds simply to the β-decay instability. The analogous point for the + branch in the case of neutron matter is called the point of π_s^+ condensation in Ref. 3. If there is no π condensate in the nucleus ^{40}Ca, i.e., $g' > g'_0$, then it follows from the fact that ^{40}Ca is stable against β decay that the constant g' in the amplitude $\mathscr{F}$ must satisfy the inequality $g' > g'_1$.

In Fig. 7, the analogous curves for the physical branches are shown for different J^π. It can be seen that everything we have said remains true for the other J^π, and the charged branches are obtained from the neutral branches by a shift along the vertical by $\Delta\mu$. Note the very different slope of the curves for the modes of different parities. This is due to the fact that in the case of negative parity a contribution to the

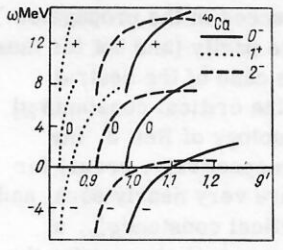

FIG. 7. Dependence of the energies of the first excited states with $J^\pi = 0^-$, 1^+, and 2^- in ^{40}Ca on g'.

propagator $A(r_1, r_2; \omega)$ is made by transitions between neighboring shells, whereas in the case of positive parity transitions through a shell contribute. We shall show how this happens for the example of the neutral channel. At low frequencies, the position of the level ω_{J^π} for given J^π can be found from the formula $\omega^2_{J^\pi} = C_{J^\pi}/B_{J^\pi}$, where C_{J^π} is the rigidity for the mode J^π, and B_{J^π} is the corresponding mass coefficient. In this region, C_{J^π} is small and at $g' = (g'_{\text{cr}})_{J^\pi}$ it vanishes, whereas the mass coefficient is not small and can be assumed constant. The values of C_{J^π} are determined basically by summation over states far from the Fermi surface, as a consequence of which the difference between the critical constants $(g'_{\text{cr}})_{J^\pi}$ is small. But states near the Fermi surface make an appreciable contribution to the mass coefficients B_{J^π}, so that, for example, B_{0^-} is appreciably greater than B_{1^+}, and, since the slope of the $\omega_{J^\pi}(g')$ curves is determined by the mass coefficients, the curve for 1^+ is much steeper than for 0^-.

For the nucleus ^{208}Pb, the picture is fundamentally the same. However, here isotopic invariance is broken rather strongly. Therefore, the charged branches (Fig. 8) are shifted relative to the neutral branches (at the same J^π) along the horizontal, and all three branches have very different profiles. Note that the displacement of the charged branches along the vertical is here appreciably less than in ^{40}Ca. This is due to the circumstance that in ^{208}Pb the Coulomb energy and the symmetry energy of the quasiparticles almost exactly compensate each other.

As in the neutral channel, the charged branches in ^{208}Pb are divided into two parity groups, but these groups change places. In Fig. 8, this is illustrated for the example of the 0^- and 1^+ modes; for the other modes, the relative disposition of the branches is the same. In ^{208}Pb, the population by neutrons and protons

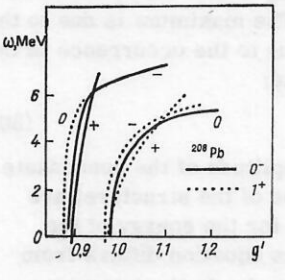

FIG. 8. Positions of the first states with $J^\pi = 0^-$ and 1^+ in ^{208}Pb as functions of g'.

differs by just one shell, so that for the charged channel the minimal energy differences in the propagator arise for the modes of positive parity (and not for those with negative parity, as in the case of the neutral channel). At the same time, the critical constants g_0' and g_1' (at which, in the terminology of Ref. 3, the "pairing" and π_s^+ instability, respectively, occur) for the modes of positive parity are very nearly equal and virtually coincide with the critical constant g_{cr}', at which instability occurs in the neutral channel for the modes with negative parity.

These considerations show that the nature of the π condensation in light and heavy nuclei may be very different. When g' decreases (the density increases) in light nuclei, the first mode to become unstable is the 0^- mode, and the influence of the other modes on its condensation can be ignored. In heavy nuclei, the situation resembles that in an infinite system, in which all modes become unstable simultaneously, though here too shell effects lead to a separation of the instability points depending on the parity. Thus, for the neutral channel in ^{208}Pb all the negative-parity modes condense before the positive-parity modes, while for the charged channels the situation is reversed.

3. IS THERE A π CONDENSATE IN NUCLEI?

In his very first papers on the problem of π condensation, Migdal discussed the possible existence of a π condensate in nuclei. At the first glance, such a conjecture appears to contradict all the experience of nuclear physics. However, analysis showed that a π condensate of small amplitude has a weak influence on the majority of nuclear properties. Moreover, it is difficult to find phenomena sensitive to the presence of a condensate and such that analysis of them would establish whether a condensate is present.

The physical picture of the π condensate is formulated in the language of the pion field. We are in fact speaking of excitations of the medium that have pion symmetry and are a superposition of pions, particle–hole excitations, and Δ-isobar–hole excitations. The π condensate is a system of standing waves of such "pions." In other words, π condensation corresponds to the occurrence of a periodic spin–isospin structure, and if it is to be revealed we require phenomena in which such structure if manifested.

One such phenomena is the elastic scattering of electrons by nuclei.[33] The existence of a π condensate must lead to an additional maximum in the differential cross section $(d\sigma/d\Omega)_{el}$ for scattering of fast electrons at momentum transfers $k \approx 3$ F^{-1}. The maximum is due to the fact that the π condensate leads to the occurrence in the nucleus of a periodic pion field:

$$\varphi = a \sin k_0 z, \tag{30}$$

where the constants a (the amplitude of the condensate field) and k_0 ($1/k_0$ is the period of the structure) are determined from the equation for the energy of the pions in nuclear matter.[3] This equation differs from (25) by the addition of the term due to the interaction of the pions with each other. In the second order in the amplitude a, there is a correction to the density:

$$\delta n(r) = n_0(r)\, \xi^2 \cos 2kz, \tag{31}$$

where

$$\xi^2 = 3f^2 k_0^2 a^2 / 16 \varepsilon_F^2. \tag{32}$$

In the Born approximation, the electric form factor of the nucleus acquires the correction

$$\delta F(k) = -\xi^2 \sin(k - 2k_0) R / (k - 2k_0) R, \tag{33}$$

which has a maximum at $k = 2k_0$ of width $\Delta k \sim 1/R$. Accordingly, at $k \sim 2k_0 \approx 3$ F^{-1} (the calculations of Ref. 3 give $k_0 \approx 1.5$ F^{-1}) an additional maximum must occur in the cross section.

A fair body of data has by now been accumulated on the cross sections of ee' scattering in the considered region of k. There have also been a considerable number of calculations of these cross sections.[34-36] All the calculations differ rather strongly (by up to a factor 2) from the experiments at $k \gtrsim 2$ F^{-1}. However, the nature of these discrepancies is different, namely, the differences between the theoretical and experimental cross sections increase monotonically with increasing k and do not have a clear maximum in the region of $k \approx 3$ F^{-1}. They are most probably due to the circumstance that at these large momentum transfers the differences between the particles and quasiparticles in the nuclei begin to have an influence.[36] Thus, although the difficulties in the theoretical description of the data on electron scattering at the present time prevent us drawing the conclusion that there is no π condensate in nuclei, the absence of a clear maximum in the electron-scattering cross section at $k \approx 3$ F^{-1} is an argument against a π condensate rather than for it.

A second phenomenon, discussed by Migdal[3] and Dmitriev,[8] is the doubling of levels if a π condensate is present. The doubling occurs for the following reason. Since the pion field is pseudoscalar, it follows from parity conservation that its expectation value in a given state of the nucleus must vanish. In the case of π condensation, the mean square of the condensate field must have a large macroscopic value. Then the field operator $\hat{\varphi}$ can be represented[3] in the form $\hat{\varphi} = \hat{q}\Psi(r)$, where $\Psi(r)$ determines the coordinate dependence of the pion field, and q is a collective coordinate, proportional to the amplitude of the condensate field and a pseudoscalar. Thus, in the case of a condensate of 0^- symmetry $\hat{q} \sim \sigma \cdot n$.[8] From the Hamiltonian of the system, we can separate a collective part, which has the form of an anharmonic oscillator with the potential (Fig. 9)

$$U(q) = -\omega_0^2 q^2/2 + \lambda_1 q^4/4, \tag{34}$$

where ω_0 and λ_1 are constants (ω_0^2 is the minimum of $\omega^2(k)$, and $\lambda_1 \sim \lambda/V$,[1)] where λ is the effective interaction constant of two condensate pions, and V is the volume of the system). The expansion of $U(q)$ near the points $\pm q_0$ has the form of an oscillator well: $U_\pm(q) = -\omega_0^4/4\lambda + \omega_0^2(q \mp q_0)^2$. We denote by $\chi_0^\pm$ the solutions in these wells, respectively. Obviously, $\langle \chi_0^{+,-} | \hat{q} | \chi_0^{+,-} \rangle$

[1)] For a two-dimensional condensate, $\lambda_1 = 3\lambda/2V$.

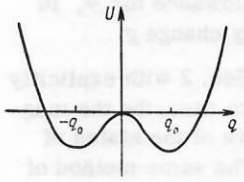

FIG. 9. Potential of the equation for the collective wave function $\chi(q)$ [see (34)].

$=\pm q_0$, i.e., these states do not have definite parity. In the case of a low barrier penetrability, solutions with definite parity are the symmetric and antisymmetric combinations of $\chi_0^{\pm}$:

$$\chi_0^{s,a}=\frac{1}{\sqrt{2}}(\chi_0^{+}\pm\chi_0^{-}). \tag{35}$$

Here, χ_0^s corresponds to the ground state (0^+) of the nucleus, and χ_0^a to an excited state (0^-). The energy of the antisymmetric level can be readily calculated in the quasiclassical approximation[3]:

$$\Delta E_{0^-}=\frac{\omega_0\sqrt{2}}{\pi}\exp\left(-\frac{\pi\omega_0^2}{4\lambda_1}\right). \tag{36}$$

Since $\lambda_1 \sim 1/V$, this quantity is exponentially small in a large system, and in the limit of an infinite system the two states are degenerate. To estimate ΔE, Migdal[3] took the values $\omega_0^2=0.2m_\pi^2$ and $\lambda=10$, which gives $\Delta E=28e^{-1.0A/100}$ MeV. For $A=208$, we have $\Delta E\approx 4$ MeV. Thus, in the ^{208}Pb nucleus at $\lesssim 4$ MeV above the ground state there must be a 0^- state having a similar wave function. Such a state is very collective and must be strongly excited in reactions capable of inducing a $0^+\to 0^-$ transition (for example, in nucleon scattering). A similar doubling must occur for the other nuclear states, i.e., ≈4 MeV above the system of "ordinary" nuclear levels there must be a band of states of opposite parity which overlap strongly with their "partners." The ^{208}Pb spectrum has been well studied up to the single-particle threshold (~7–8 MeV), and it does not contain any levels whose nature cannot be understood from the point of view of the simple quasiparticle picture. In our view, this fact is a strong argument against the existence of a condensate in nuclei. However, one can ask how realistic is the estimate for ΔE if a π condensate exists in nuclei. Now although this estimate does contain some uncertain factors, it is probably an upper bound (for example, the estimate of Ref. 3 for ^{208}Pb gives $\Delta E\approx 1$ MeV). Finally, if one supposes that $\Delta E > 8$ MeV and that the 0^- level is in the continuum, it should still be manifested as a very collective (collectivity of order A) giant 0^- resonance, which is not found.

Finally, the last phenomenon that we shall discuss in this section is the single-nucleon width of the levels of π atoms or, which is physically almost the same thing, the probability of single-nucleon capture of slow pions.

In Ref. 7, and also in Ref. 37, it was shown that this process is critical from the point of view of establishing whether a π condensate is present or absent in nuclei.

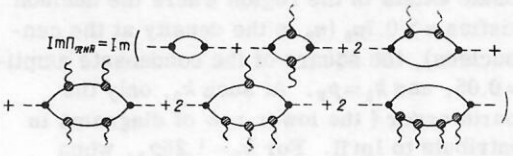

FIG. 10. Skeleton diagrams of the pion polarization operator in nuclear matter that determine the probability of single-nucleon capture. The wavy line denotes the static condensate field. At the hatched vertices, the renormalization effects due to the spin-dependent Fermi-liquid interaction are taken into account.

In infinite nuclear matter, such a process is forbidden by the energy and momentum conservation laws if a π condensate is absent. In finite nuclei, nonconservation of the momentum ($\sim 1/R$, where R is the radius of the nucleus) permits this process, but to a very small extent. In the presence of a π condensate, single-nucleon capture also becomes possible in infinite matter. This is because the periodic structure of the spin–isospin density permits "transfer" processes, in which the nucleon momentum p changes by $\mathbf{p}\pm\mathbf{k}_0$ ($\mathbf{k}_0$ is the "momentum" of the condensate). This effect leads to an appreciable increase (by about two orders of magnitude) in the probability of single-nucleon capture in finite nuclei as compared with the case without a condensate. In Ref. 7, this effect was considered for a weak condensate field, when perturbation theory with respect to it can be used. The probability of single-nucleon capture is proportional to the imaginary part of the pion polarization operator $\Pi_{\pi N\bar{N}}(\omega,k)$. The skeleton graphs for Π calculated in Ref. 7 are shown in Fig. 10. Here, the broken lines represent the "external" pion with frequency ω and wave vector k, and the wavy line represents the static condensate field with momentum k_0 and amplitude a. Because of the symmetry of the condensate field $(\sigma\cdot\mathbf{k}_0)\tau$, the expansion of Π is with respect to only even powers of the amplitude. The need to take into account terms of fourth order in a is due to the circumstance that the second-order terms contribute to Im Π only if $k_0 > 1.1p_F$.

In Table II, we give the results of the calculations in Ref. 7 of the relative probability W_1 ($W_1=\Gamma_1/\Gamma$, where Γ_1 is the single-nucleon and Γ the total width) of single-nucleon capture of pions from different mesoatomic levels of various nuclei from ^{40}Ca to ^{238}U. The calculation was made both without and with condensate. In the latter case, the following assumptions were made:

TABLE II. Partial probability of absorption of π^- mesons by nuclei with emission of a single nucleon in a situation with and without pion condensate.[7]

Element	Level of π atom	Relative probability of emission of a nucleon, %		Element	Level of π atom	Relative probability of emission of a nucleon, %	
		without condensate	with condensate			without condensate	with condensate
^{238}U	$5g$	0.13	4	^{60}Ni	$3d$	0.50	8
	$4f$	0.08	4		$2p$	0.28	4.5
^{208}Pb	$4f$	0.12	5	^{40}Ca	$3d$	0.36	7
^{119}Sn	$3d$	0.30	5		$2p$	0.16	4

The condensate exists in the region where the nucleon density satisfies $n > 0.7n_0$ (n_0 is the density at the center of the nucleus), the square of the condensate amplitude is $a^2 = 0.05$, and $k_0 = p_F$. At such k_0, only the terms of fourth order (the lower row of diagrams in Fig. 10) contribute to Im Π. For $k_0 = 1.25p_F$, when second-order processes are allowed, Im Π is increased by about four times. Finally, allowance in Π for terms in which there is virtual production of the Δ isobar leads to an increase in the numbers in the last column of Table II by about a further 1.5 times. Thus, when a π condensate exists in the nuclei, the values in the last column are a lower bound for W_1. They are about two orders of magnitude greater than the values in the absence of a condensate.

Unfortunately, there have been very few measurements of the single-nucleon widths. In Ref. 38, Anderson *et al.* measured the energy spectrum of neutrons with energies up to 150 MeV in reactions with the capture of a slow pion by Pb and U nuclei. The estimate $W_1 \approx 10^{-3}$ (true, with a large error) was given. In Ref. 39, the value $W_1 \approx 10^{-3}$ was also obtained for the reaction ^{165}Ho(π^-, xn). Such values agree well with the assumption that there is no condensate in nuclei. If one assumes that there is nevertheless a condensate, then for its amplitude very small values are permitted: $a^2 < 5\times10^{-3}$ if $k_0 = p_F$, and $a^2 < 4\times10^{-4}$ if $k_0 = 1.25p_F$. An even stronger restriction can be deduced from the data of Ref. 6, in which a probability less than 10^{-5} was obtained for the reaction ^{181}Ta$(\pi^-, n)^{180m}$Hf ($T_{1/2} = 5.5$ h, $J^\pi = 8^-$). However, the structure of the final state is evidently such that the reaction is determined by the surface region, where a condensate does not exist. These strong limits on the amplitude of the condensate field indicate that there is probably no condensate in nuclei. In any case, a condensate with such a small amplitude does not admit description in terms of a classical field, as assumed in Refs. 3 and 7, i.e., it is a much more complicated entity. However, the main circumstance which here makes it impossible to conclude definitely that a condensate is absent is the insufficient completeness of the experimental data.

The situation with regard to the existence of a π condensate in nuclei can be summarized as follows:

1. No clear indication of the existence of a condensate is known.

2. There are no absolutely rigorous proofs that it does not exist in nuclei.

3. There are some nonrigorous indications that there is no π condensate.

4. PARAMETERS OF THE EFFECTIVE INTERACTION

In the first estimates of the proximity of nuclei to the point of π condensation,[1] the value of the constant g' found in the theory of finite Fermi systems by analyzing the experimental data without explicit separation of the amplitude of one-pion exchange $\mathcal{F}_\pi$ was used. However, as a rule not only small but also large ($\sim p_F$) momentum transfers k are represented in the analyzed phenomena. Therefore, explicit allowance for $\mathcal{F}_\pi$ in the analysis of such phenomena may change g'.

In Refs. 11–13, the equations of Sec. 2 with explicitly separated amplitude $\mathcal{F}_\pi$ were used to describe the magnetic characteristics and the spectra of the states of anomalous parity ($0^-, 1^+, 2^-, \ldots$). The same method of exact solution of the equations for finite Fermi systems in the coordinate space as in the investigation of the π-condensate instability was used. From the analysis, the parameters of the amplitude $\mathcal{F}$ were determined and their values were found to be close to the critical values.

Spectra of the states of anomalous parity. The problem of finding the spectra of the states of particle–hole nature is the most natural for determining the parameters of the effective interaction. This is because the level shift relative to the position given by the independent-particle model is proportional to the interaction amplitude Γ and does not contain other unknown factors such as those, for example, that occur in the local quasiparticle charge e_q in the calculation of the magnetic moments or $B(ML)$.

However, in the spectral problem we come right up against the question of the approximation of $\mathcal{F}$ by the comparatively simple form (4), (10), and (11), in which, in particular, the one-pion exchange amplitude $\tilde{\mathcal{F}}_\pi$ in the transverse channel (in the scattering channel) is approximated by a local function and assumed to be included in $\mathcal{F}_0$. Such an operation is justified in the equation for the effective field, in which, as a rule, $\tilde{\mathcal{F}}_\pi(q)$ is integrated over a wide ($\sim 2p_F$) range of momenta q transferred in this channel. The situation is the same in the eigenfrequency equation (28) when the state $|s\rangle$ is collective. By a collective state, we mean one in whose transition density

$$\rho_{tr}(\mathbf{r}) = \int A(\mathbf{r}, \mathbf{r}'; \omega_s)\, v_s(\mathbf{r}')\, d\mathbf{r}' = \sum_{\lambda\lambda'} \rho^{tr}_{\lambda\lambda'} \varphi^*_\lambda(\mathbf{r})\, \varphi_{\lambda'}(\mathbf{r}) \qquad (37)$$

there are no distinguished components $\rho^{tr}_{\lambda\lambda'}$. The matrix elements $\rho^{tr}_{\lambda\lambda'}$ are normalized as follows:

$$\sum_{\lambda\lambda'} (n_\lambda - n_{\lambda'})\, |\rho^{tr}_{\lambda\lambda'}|^2 = -1. \qquad (38)$$

For the collective states, all $|\rho^{tr}_{\lambda\lambda'}| \ll 1$. But the majority of states that we consider are not collective, and for them the sum (37) has a few (generally just one) distinguished components, and the others are each separately small, so that only their coherent superpositions are important. In such cases, the fine details of $\mathcal{F}$ frequency come into play, especially one-pion exchange in the transverse channel, which makes the analysis much harder. We note that the separation from $\mathcal{F}$ of a term $\tilde{\mathcal{F}}_\pi$ with "bare" pion, as is done in Ref. 40, does not solve the problem, since it is in fact

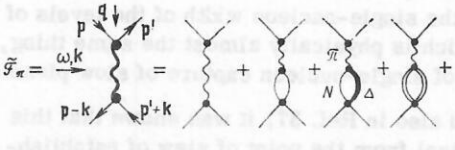

FIG. 11. Amplitude of one-pion exchange in the transverse channel (scattering channel).

a "fat" pion (Fig. 11), which differs strongly from a vacuum pion because of the polarization of the medium, that is exchanged. In the general case, the correct separation of $\tilde{\mathscr{F}}_\pi$ is a difficult problem.

To describe the noncollective states, it is convenient to represent the particle–hole propagator A in Eq. (28) in the form

$$A(\mathbf{r}_1, \mathbf{r}_1', \mathbf{r}_2, \mathbf{r}_2'; \omega) = \sum_{\lambda\lambda'} \frac{n_\lambda - n_{\lambda'}}{\varepsilon_\lambda - \varepsilon_{\lambda'} - \omega} \varphi_\lambda(\mathbf{r}_1) \varphi_{\lambda'}^*(\mathbf{r}_1') \varphi_\lambda^*(\mathbf{r}_2) \varphi_{\lambda'}(\mathbf{r}_2') \tag{39}$$

and make a decomposition into the sum

$$A = A_0 + A', \tag{40}$$

where A_0 includes only the terms that make a dominant contribution to $\rho^{\mathrm{tr}}(\mathbf{r})$. Then from (28), we obtain

$$v_s = \Gamma'(\omega_s) A_0(\omega_s) v_s, \tag{41}$$

where

$$\Gamma'(\omega_s) = \mathscr{F} + \mathscr{F} A'(\omega_s) \Gamma'(\omega_s). \tag{42}$$

To be specific, we consider the most common case when just one particle–hole state $|12\rangle$ is represented in A_0. We introduce the notation

$$\left.\begin{aligned} &\omega_{12} = \varepsilon_1 - \varepsilon_2, \quad (v_s)_{12} \\ &= \int v_s(\mathbf{r}_1, \mathbf{r}_2)\, \psi_{12}^{JM}(\mathbf{r}_1, \mathbf{r}_2)\, d\mathbf{r}_1 d\mathbf{r}_2, \\ &\psi_{12}^{JM}(\mathbf{r}_1, \mathbf{r}_2) = \sum_{m_1 m_2} (-1)^{j_2 - m_2} C_{j_2 m_2 j_1 m_1}^{JM} \varphi_{j_1 m_1 l_1 n_1}(\mathbf{r}_1)\, \varphi_{j_2 - m_2 l_2 n_2}^*(\mathbf{r}_2), \\ &[\Gamma_J'(\mathbf{r}_1, \mathbf{r}_2)]_{12} = \int \Gamma'(\mathbf{r}_1, \mathbf{r}_2, \mathbf{r}_3, \mathbf{r}_4; \omega_s)\, \psi_{12}^{JM}(\mathbf{r}_3, \mathbf{r}_4)\, d\mathbf{r}_3 d\mathbf{r}_4 \end{aligned}\right\}$$

and

$$[\Gamma_J']_{12}^{12} = \int [\Gamma'(\mathbf{r}_1, \mathbf{r}_2)]_{12}\, \psi_{12}^{JM}(\mathbf{r}_1, \mathbf{r}_2)\, d\mathbf{r}_1 d\mathbf{r}_2.$$

Then it follows from (41) that

$$\omega_s = \omega_{12} + [\Gamma_J'(\omega_s)]_{12}^{12} \tag{43}$$

and

$$v_s(\mathbf{r}_1, \mathbf{r}_2) = [\Gamma_J'(\mathbf{r}_1, \mathbf{r}_2)]_{12} (v_s)_{12} / (\omega_s - \omega_{12}). \tag{44}$$

Equations (42)–(44) are completely identical to the original (28). However, as a rule, they are much more convenient, since, first, they admit a simple iterative solution,[41] and, second, they are well adapted for qualitative estimates and approximate calculations.

Thus, for noncollective states the energy shift $\Delta\omega = \omega_s - \omega_{12}$ is equal to the individual matrix element $[\Gamma_J']_{12}^{12}$, which is a weak function of the frequency ω near ω_s, the estimate for it giving $\sim[\mathscr{F}_J]_{12}^{12} \lesssim \varepsilon_F A^{-2/3}$. Another criterion for a state to be noncollective is a small value of $\Delta\omega$, which is the case for almost all the states of anomalous parity in ^{208}Pb (Table III). The matrix element $[\Gamma_J'(\omega_s)]_{12}^{12}$ is related in a simple manner to the matrix elements $[\Gamma_I']_{1\tilde{1}}^{2\tilde{2}}$ with fixed angular momentum I in the transverse channel (Fig. 12):

$$\Gamma_J = \sum_I \begin{Bmatrix} j_1 j_2 J \\ j_2 j_1 I \end{Bmatrix} (2I+1)(-1)^{j_1+j_2+I+J} \Gamma_I. \tag{45}$$

In general, the summation over I leads to a certain averaging over the momentum q, which predetermines an advantage of the annihilation channel over the scattering channel in the cases when the angular momenta j_1 and j_2 are both large, so that in (45) the summation is over a large number $(2\min\{j_1, j_2\} + 1)$ of angular momenta I. But if either of the angular momenta j_1 and j_2 is small, the number of terms in the sum over I is also small (for example, for $j = \frac{1}{2}$ only $I^\pi = 0^+$ and 1^+ are possible), and then it is *a priori* quite unclear in which channel the equation for Γ must be developed. In Ref. 11, a careful analysis was made of the anomalous-parity states in ^{208}Pb with a view to finding "pure" cases in which averaging over q occurs to a sufficient extent in the transverse channel for the approximation (4) for $\mathscr{F}$ to be fully admissible. It was found that this is the case for the states 2_1^-, 0_1^-, and 1_2^+ (true, the experimental situation with regard to the 1^+ levels is not entirely clear). The results of calculation of ω_s for these states are given in the upper part of Table III. The calculated variant with $g = 0.65$ is taken from Refs. 12 and 41. To investigate the sensitivity of the results to the isoscalar constant g, a calculation was also made for $g = 0.3$. It can be seen that in the majority of cases the dependence on g is very weak, although overall the agreement with experiment for $g = 0.3$ is somewhat better. For both values of g, the experimental data are reproduced best for $g' \approx 0.80$–0.85, which is fairly close to the point of π condensation (we recall that for $\alpha = 0$ and $\zeta_s = 0.05$ the instability arises at $g'_{\mathrm{cr}} = 0.70$).

Cases are known when the distribution over the momentum k in the "direct" channel is more or less smooth but it is not over the momentum q in the transverse channel. It is then more expedient to use the expansion (45) and develop the equation for Γ_I in the transverse channel. Such a program without allowance for one-pion exchange was carried out in Ref. 42 for, in particular, the doublet $(5^+, 4^+)$ in ^{209}Bi, which has the pure configuration $|1h_{9/2}^{p} 3p_{1/2}^{n}\rangle$. The center of gravity of the doublet is determined by the matrix element $\Gamma_{I^\pi=0^+}$, and the splitting by the matrix element $\Gamma_{I^\pi=1^+}$. The experimental value of this splitting is $\Delta E = -77$ keV, and the calculation of Ref. 12 for $g = 0.3$, $\alpha = 0$, $\zeta_s = 0.05$, and $g' = 0.85$ gives $\Delta E = -74$ keV. Thus, this set of constants describes rather well all the "pure" cases.

In the lower part of Table III, we give the results of calculations for the other anomalous-parity states in lead. It can be seen that the best agreement with experiment is generally obtained for the same sets of constants near the critical sets, although in individual

TABLE III. Energies of particle–hole states of anomalous parity in ^{208}Pb.

J^π	ω_{exp}, MeV	ω_{12}, MeV	ω_{theor}, MeV [$\alpha = 0, \zeta_s = 0.05$]				
			$g = 0.65$			$g = 0.3$	
			$g' = 0.80$	$g' = 0.85$	$g' = 1.00$	$g' = 0.80$	$g' = 0.85$
2_1^-	4.23	4.00	4.13	4.27	4.39	4.04	4.20
0_1^-	5.28	5.46	4.80	5.23	5.51	4.64	5.15
1_2^+	7.2 (?)	5.57	6.97	7.07	7.27	7.05	7.24
2_2^-	5.04	5.00	4.97	5.13	5.19	4.85	5.07
4_1^-	3.48	3.43	3.51	3.52	3.54	3.48	3.50
4_2^-	3.92	4.00	4.05	4.09	4.12	4.01	4.06
4_3^-	4.13	4.21	4.12	4.20	4.28	4.10	4.17
6_1^-	3.99	4.00	4.04	4.04	4.05	4.02	4.03
6_2^-	4.21	4.21	4.22	4.24	4.27	4.19	4.22
6_3^-	4.39	4.33	4.34	4.42	4.49	4.27	4.36
12_1^-	6.42	6.49	—	—	—	6.63	6.65
12_2^-	7.06	7.22	—	—	—	7.35	7.45

cases the positions of the levels are not reproduced so well as for "pure" states.

We note that in light nuclei (^{12}C, ^{16}O) the single-particle angular momenta j_1 and j_2 in (45) are small, so that the direct solution of (28) in the annihilation channel[40] yields little information. We shall demonstrate this for the example of the first two 0^- states in ^{16}O (Ref. 43). The level 0^- ($T=1$; 12.78 MeV) is frequently discussed in connection with the question of the proximity of nuclei to the π-condensate instability.[44,45]

Its energy is 360 keV higher than the value $\omega_{12}=12.42$ MeV given by the independent-particle model. A straightforward calculation in the direct channel with the same set of parameters as for ^{208}Pb lowers the level by $\Delta\omega\approx-1$ MeV. This is because in this case irregular components of the amplitude in the transverse channel play an important part. An indication of their importance can be deduced, in particular, from the fact that the level 0^- ($T=0$) is shifted downward by the interaction, and appreciably ($\Delta\omega_{exp}=-1.2$ MeV), whereas the isoscalar spin part of the amplitude $\mathcal{F}$ is evidently repulsive.[26] In Ref. 43, an alternative calculation was made of the positions of these levels using the equation for Γ in the transverse channel (note that in this case the level shift is determined not only by the spin components of $\mathcal{F}$ but also by the scalar components f and f', which are rather well known[20]). The calculation yielded the correct order of the levels, the level with $T=1$ being raised and that with $T=0$ lowered. However, in both cases the shift was too large: $\Delta\omega_{0^-,T=1}=+2.6$ MeV, $\Delta\omega_{0^-,T=0}=-4.3$ MeV. Evidently, simultaneous allowance for both channels will make it possible to describe both levels correctly with the same interaction parameters as in the heavy nuclei, although the ^{16}O nucleus is too light for the reliable use of the many-body methods on which the theory of finite Fermi systems is based, so that a certain variation of the parameters on the transition from ^{208}Pb to ^{16}O is quite admissible. Whatever the case, it appears to us incorrect to rely on calculations for the ^{16}O and ^{12}C nuclei[40] in attempting to establish how close nuclei are to the point of π condensation.

Wave functions of anomalous-parity states. For the three states 2^-_1, 4^-_1, and 6^-_1 in ^{208}Pb phenomenological "wave functions" are known, i.e., the components $\rho^{tr}_{\lambda\lambda'}$ of the transition density (37), which for these states could be extracted directly from data on β and γ transitions.[46] In such a procedure, of course, one can determine only the principal components $\rho^{tr}_{\lambda\lambda'}$, one of which is of order unity, $\rho_{12}\sim1$, several are of order 0.1, and the remainder, which are very small, are

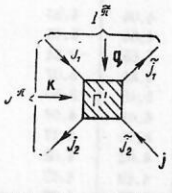

FIG. 12. Nucleon interaction amplitude that determines the shift of the noncollective level with respect to the differences between the energies of the particle–hole levels j_1 and $\tilde{j}_2$.

TABLE IV. Principal components $\rho_{\lambda\lambda'}$ of the transition densities of the first anomalous-parity states in ^{208}Pb.

J^π		$\lvert\rho^{tr}_{\lambda\lambda'}\rvert$			
2^-_1	Experiment Theory	0.98 0.95 (1)	0.21 0.24 (6)	0.05 0.11 (8)	0.03 0.04 (7)
4^-	Experiment Theory	0.92 0.98 (2)	0.24 0.09 (3)	0.12 0.04 (9)	0.06 0.05 (5)
6^-	Experiment Theory	0.87 0.99 (1)	0.35 0.01 (9)	0.33 0.08 (4)	0.10 0.09 (3)

Note. In the brackets, the numbers of the particle–hole configurations, which are numbered as follows, are given: (1) $2g^n_{9/2}-2f^{-n}_{5/2}$; (2) $2g^n_{9/2}-3p^{-n}_{1/2}$; (3) $2g^n_{9/2}-3p^{-n}_{3/2}$; (4) $1i^n_{11/2}-3p^{-n}_{1/2}$; (5) $2g^n_{9/2}-2f^{-n}_{7/2}$; (6) $3d^n_{5/2}-3p^{-n}_{1/2}$; (7) $3d^n_{5/2}-2f^{-n}_{5/2}$; (8) $3d^n_{5/2}-3p^{-n}_{3/2}$; (9) $1h^p_{9/2}-1d^{-p}_{3/2}$.

ignored. In Ref. 41, the components $\rho^{tr}_{\lambda\lambda'}$ were calculated for a set of constants (Table IV) chosen from analysis of spectra. It can be seen that the principal components ρ_{12} are well reproduced, but this is not surprising, since their proximity to 1 depends little on the details of $\mathcal{F}$. The components $\rho^{tr}_{\lambda\lambda'}$ next in magnitude are much more sensitive to the choice of the parameters of $\mathcal{F}$.

It can be seen from comparison with Table III that there is a correlation between the correctness in the description of the spectra of the states and the accuracy in the reproduction of their wave functions. The best reproduction is obtained for the wave function of the state 2^+_1, which, as we noted above, is "pure" in the sense that the irregularities of the amplitude in the transverse channel are not important for it. Overall, one achieves a satisfactory description of the principal components of the transition densities of the considered states, which is an additional indication that the employed interaction is realistic.

Magnetic characteristics of nuclei. In Ref. 13, the method described above was applied to the analysis of the magnetic moments and probabilities of M1 transitions.

The effective single-particle operator of the magnetic moment (in nuclear magnetons) has the form

$$\mu^\alpha=\tfrac{1}{2}[1+(1-2\zeta_l)\tau_3]\,j^\alpha+V[\mu^\alpha_s], \tag{46}$$

where $j^\alpha=l^\alpha+\frac{1}{2}\sigma^\alpha$, and l^α is the operator of the orbital angular momentum. The spin part μ^α is determined by the equation

$$V[\mu^\alpha_s]=\hat{e}_q\mu^\alpha_s+\mathcal{F}AV[\mu^\alpha_s]; \tag{47}$$

$$\mu^\alpha_s=\tfrac{1}{2}\left[\left(\gamma_p-\tfrac{1}{2}\right)(1+\tau_3)+\gamma_n(1-\tau_3)\right]\sigma^\alpha, \tag{48}$$

where $\gamma_p=2.793$, $\gamma_n=-1.913$, and $\hat{e}_q$ is the operator of the local quasiparticle charge relative to the field μ_s:

$$\hat{e}_q\mu_s=\tfrac{1}{2}(\gamma_p+\gamma_n-1/2)\,\sigma^\alpha+\tfrac{1}{2}[(\gamma_p-\gamma_n-1/2)(1-2\zeta_s)+\zeta_l]\,\sigma^\alpha\tau_3+\hat{e}^t_q. \tag{49}$$

Here, ζ_s and ζ_l are known constants in the theory of finite Fermi systems,[26] and $\hat{e}^t_q$ is the tensor part of $\hat{e}_q$ induced by the velocity and noncentral forces. The

amplitude $\mathcal{F}$ is determined by the expressions (4), (10), and (11).

The analysis of the magnetic moments and $B(ML)$ is difficult because of the complicated structure of the operator $\hat{e}_q$ of the local charge. In the expression (49), the constants ζ_s and ζ_l are known relatively well. The constant ζ_s ensures suppression of the spin gyromagnetic ratio, and also of the probabilities of Gamow–Teller β transitions in mirror nuclei with closed spin–orbit doublets, for which the integral term in Eq. (47) is absent. The constant ζ_l is needed to reconcile the magnetic moments of states with large l. The operator $\hat{e}_q$, in contrast to the first terms in (49), contributes to the l-forbidden M1 transitions with $\Delta l = 2, \Delta j = 1$. At the present time, its structure has not been fully elucidated. In an infinite system, $\hat{e}_q^t$ is proportional to $(\sigma \cdot p)p_\alpha$ [the term $\sim(\sigma \cdot k)k_\alpha$ does not contribute to μ^α]. In a finite system, there are also surface terms containing the derivatives of the density n [for example, $\sim(\sigma \cdot \nabla n)r_\alpha$]. In particular, they are induced by the spin–orbit interaction.[47,48]

The main aim of the analysis was to establish the extent to which the magnetic characteristics of nuclei are sensitive to allowance for $\mathcal{F}_\pi$ and, in particular, to the proximity of nuclei to the point of π condensation. Therefore, we took the constants $\zeta_s = 0.05$ and $\zeta_l = -0.04$ from Ref. 26, in which they were determined by analyzing the magnetic moments of a large number of nuclei, and we ignored the contribution of $\hat{e}_q^t$. The constant α in (10) was set equal to zero. To simplify the calculations (no pairing and no low-lying 2^+ levels) we restricted ourselves to neighbor nuclei of ^{208}Pb.

To establish the part played by one-pion exchange, we compared the results of calculations with and without introduction of the amplitude $\mathcal{F}_\pi$. The results of the calculations are given in Tables V and VI. The general result of the analysis is as follows. First, the inclusion of $\mathcal{F}_\pi$ has little influence on the magnetic moments and the B(M1) of allowed transitions. Second, these quantities depend weakly on g and g' in the intervals $g = 0.4$–0.8, $g' = 0.7$–1.0. An appreciable dependence on g' arises only near the critical value $(g'_{cr})_{1^+} \approx 0.6$ for the mode 1^+ (see Table I), i.e., in the region that is forbidden if there is no π condensate [since $(g'_{cr})_0 = 0.7$]. Finally, the probabilities of l-forbidden M1 transitions are sensitive to $\mathcal{F}_\pi$ and to the value of g'. This fact was noted in Ref. 11, in which Eq. (47) was solved approximately, and the anomalously large (compared with standard calculations in the theory of finite Fermi systems) B(M1) values of the l-forbidden transitions were explained by the proximity of nuclei to the point of π condensation. The exact calculation of Ref. 13 did not confirm this conclusion, and the necessary enhancement of B(M1) occurs only in the "forbidden" region $g' < 0.7$.

TABLE V. Magnetic moments (in nuclear magnetons) of the ^{208}Pb neighbor nuclei for different values of the constants g and g' ($\zeta_s = 0.05$ and $\alpha = 0$).

Constants		State λ_0						
g	g'	$3p^{-n}_{1/2}$	$2f^{-n}_{5/2}$	$1i^{-n}_{13/2}$	$2g^{n}_{9/2}$	$3s^{-p}_{1/2}$	$1h^{p}_{9/2}$	$1i^{p}_{13/2}$
Without allowance for F_π								
0.4	1.0	0.41	0.71	−1.19	−1.30	1.91	3.69	7.97
0.8	0.6	0.46	0.84	−1.39	−1.47	2.08	3.55	8.15
	0.8	0.44	0.77	−1.29	−1.38	1.98	3.64	8.04
	1.0	0.41	0.72	−1.21	−1.31	1.89	3.72	7.95
	1.2	0.39	0.67	−1.14	−1.25	1.82	3.78	7.88
1.2	1.0	0.41	0.72	−1.22	−1.32	1.88	3.73	7.94
With allowance for F_π								
0.4	1.0	0.44	0.68	−1.20	−1.25	1.89	3.78	7.97
0.8	0.7	0.80	0.82	−1.32	−1.19	2.33	3.90	8.06
	0.8	0.53	0.74	−1.29	−1.26	2.00	3.81	8.03
	1.0	0.44	0.69	−1.21	−1.26	1.87	3.87	7.95
	1.2	0.40	0.65	−1.15	−1.22	1.80	3.83	7.88
1.2	1.0	0.44	0.70	−1.22	−1.26	1.86	3.82	7.94
Experiment		0.59	0.79	−1.00 ±0.03	−1.33 ±0.06	1.83	4.08	8.07 ±0.19

TABLE VI. B(M1) [in the units (nuc.magn.)^2] in the ^{208}Pb neighbor nuclei for different values of the constants g and g' ($\zeta_s = 0.05$ and $\alpha = 0$).

		Allowed			*l*-forbidden (× 10^3)			
g	g'	$3p^{-n}_{3/2} \to 3p^{-n}_{1/2}$	$2f^{-n}_{7/2} \to 2f^{-n}_{5/2}$	$2f^{p}_{5/2} \to 2f^{p}_{7/2}$	$3p^{-n}_{3/2} \to 2f^{-n}_{5/2}$	$1i^{n}_{11/2} \to 2g^{n}_{9/2}$	$3d^{-p}_{3/2} \to 3s^{-p}_{1/2}$	$2f^{p}_{7/2} \to 1h^{p}_{9/2}$
Without allowance for F_π								
0.4	1.0	0.38	0.43	0.94	1.78	0.08	2.02	0.47
0.8	0.6	0.50	0.59	1.19	1.56	0.12	1.81	0.28
	0.8	0.44	0.51	1.04	1.73	0.12	1.91	0.36
	1.0	0.39	0.44	0.91	1.78	0.12	2.02	0.41
	1.2	0.35	0.39	0.82	1.77	0.12	2.00	0.44
1.2	1.0	0.39	0.45	0.90	1.82	0.15	1.98	0.37
With allowance for F_π								
0.4	1.0	0.34	0.36	0.81	2.15	1.85	1.41	0.01
0.8	0.7	0.37	0.17	0.38	2.33	14.4	3.54	5.16
	0.8	0.37	0.32	0.69	0.82	5.65	2.14	0.55
	1.0	0.35	0.37	0.79	2.06	1.98	1.45	0.002
	1.2	0.32	0.35	0.76	2.15	1.00	1.39	0.09
1.2	1.0	0.35	0.38	0.77	2.02	2.04	1.46	0
Experiment		0.41 ±0.06	0.49 ±0.15	0.76 ±0.14	48 ±13	9.9 ±0.9	23 ±9	4.1 ±0.9

To explain the data on the l-forbidden transitions, a tensor term of large magnitude of the form $\sim\varkappa_t(\sigma \cdot r)r_\alpha$ was introduced in the operator $\hat{e}_q$ in a number of studies by the Jülich group.[49,50] Theoretically, the introduction of such a "charge" appears entirely unjustified, since it represents a bulk force and is moreover translationally noninvariant. In addition, its contribution in different nuclei will increase as $A^{2/3}$ with increasing A. Finally, the inclusion of such a large term in $\hat{e}_q$ leads to a discrepancy with the experimental magnetic characteristics of other nuclei. The most successful description of the l-forbidden transitions was obtained by Sadovnikova in Ref. 51, who took into account the contribution of spin–orbit forces in the Hartree–Fock method. In individual cases, the influence of low-lying collective states is also important.[52] To explain the data on the l-forbidden transitions, it is obviously necessary to take into account simultaneously all the factors listed above.

If we leave out of account the as yet not fully elucidated question of the l-forbidden transitions, the results of the calculations in Refs. 49 and 50 are close to ours and give for g and g' values in the indicated interval. The calculations of Ref. 40 with separation of one-pion exchange (in the direct and transverse channels), and also with explicit allowance for ρ-meson exchange,

also demonstrate the weak influence of these components on the majority of the magnetic characteristics of nuclei. To explain the l-forbidden transitions, a value of the constant $\varkappa_t$ even larger than in Refs. 49 and 50 was proposed in Ref. 40; moreover, it was very different for neutrons and protons.

Overall, this analysis shows that the magnetic characteristics of nuclei can be fairly well described by the interaction $\mathcal{F}$ with the chosen set of parameters, which confirms the realistic nature of the interaction we have used; as we have noted, this indicates that nuclei are near the point of π condensation. In the following section, we shall consider more closely what we mean by this and discuss its consequences.

5. PRECRITICAL PHENOMENA IN NUCLEI

The problem of π-meson condensation is frequently formulated[3] in terms of a "pion" field φ_k whose source is the distribution of the spin–isospin density of the nucleons:

$$(\omega^2 - k^2 - m_\pi^2)\,\varphi_k = if \sum_{\mathbf{p}} \psi_{\mathbf{p}}^+ (\sigma\mathbf{k})\,\tau\psi_{\mathbf{p}+\mathbf{k}}. \tag{50}$$

In their turn, the nucleon operators ψ are coupled to the field φ_k:

$$(\varepsilon - \mathcal{H}_{\mathbf{p}})\,\psi_{\mathbf{p}} = -if \sum_{\mathbf{k}} (\sigma\mathbf{k})\,\tau\psi_{\mathbf{p}-\mathbf{k}}\varphi_{\mathbf{k}}, \tag{51}$$

where $\mathcal{H}_p$ is the single-particle Hamiltonian of the quasiparticles. As a result, one obtains a system of coupled equations, which are sometimes used[16] to consider precritical phenomena in nuclei. But since the field φ_k is so strongly mixed with the particle–hole excitations of the medium, which is very different from free pions, it is in fact convenient to eliminate the field and formulate the problem in the language of an effective field acting on the nucleons. At the same time, bearing in mind that the phenomena in which we are interested occur at large wave vectors $k \sim p_F$, we can use Eqs. (18)–(26) for the effective spin–isospin field in an infinite system for qualitative estimates.

As we have seen, proximity to the point of π condensation means that the denominator of the longitudinal $\sim(\sigma\cdot\mathbf{k})k_\alpha\tau_\beta$ component of the field $V_2(k)$ at small ω and $k \sim k_0$ is small. This leads to an enhancement of V_2 in the region $k \sim k_0$. We consider first the static case. Then from (20),

$$\chi(k) = \frac{2.3k^2(1-2\zeta_s)^2}{\tilde{\omega}^2(k)} \frac{\Phi_0(k)}{(1+2g'\Phi_0(k))}, \tag{52}$$

where $\tilde{\omega}^2(k)$ is given by (25). The quantity $\chi(k)$ is the longitudinal component of the isovector magnetic permeability of nuclear matter. Near the point of π condensation, the denominator of (52) can be represented in the neighborhood of k_0 in the form

$$\tilde{\omega}^2(k) = \tilde{\omega}^2(k_0) + [\tilde{\omega}^2(k)]'_{k=k_0}(k^2 - k_0^2)^2/2, \tag{53}$$

where k_0 is determined by the condition $[\tilde{\omega}^2(k)]'_{k=k_0} = 0$ (the prime denotes differentiation with respect to k^2). For parameters near the critical set $(\alpha_{cr}, g'_{cr}, \zeta_{s\,cr})$, for which $\tilde{\omega}^2(k_0)$ vanishes, this quantity can be expanded in a series in powers of the differences $\alpha - \alpha_{cr}, g' - g'_{cr}$, and $\zeta_s - \zeta_{s\,cr}$. Thus, for one of the sets, $\alpha_{cr} = 0, \zeta_{s\,cr} = 0.05$, and $g'_{cr} = 0.63$ (see Fig. 4; the corresponding critical momentum is $k_0 = 1.33\ F^{-1}$), we obtain after variation of (25) and substitution of the numerical coefficients

$$\tilde{\omega}^2(k_0) = m_\pi^2 [1.8(\alpha - \alpha_{cr}) + 2.6(g' - g'_{cr}) + 13(\zeta_s - \zeta_{s\,cr})]. \tag{54}$$

The smallness $\tilde{\omega}^2(k_0)$ determines the enhancement factor $\chi(k)$ of the effective field at $k \sim k_0$.

There is a similar enhancement for the pion field $\varphi_k(\omega \approx 0)$. This phenomenon recalls the growth of the electric or mangetic susceptibility of a condensed medium near the critical temperature T_c in a phase transition of the second kind. Near T_c, such media are characterized by so-called critical opalescence, and in the case of a liquid this is reflected in an abrupt darkening of the material due to the growth of Rayleigh scattering of light by fluctuations of the permittivity; in the case of a ferromagnet or antiferromagnet it is reflected in an increase in the scattering of neutrons at the Bragg angles due to the growth near T_c of the fluctuations in the magnetic susceptibility.

When we consider the proximity of nuclei to the point of π condensation, nothing similar occurs, since the coefficient of enhancement $\chi(k)$ of the effective field does not undergo any fluctuations. Essentially, the refractive index of static pions increases, and not their scattering. Nevertheless, this effect has been known as critical opalescence since Ref. 16. In our view, this is not a suitable name.

The expressions (52)–(54) make more precise the sense in which we say that nuclei are close to the point of π condensation, namely, it is necessary that for $k \sim k_0$ the inequality $\chi(k) \gg 1$ hold, which, in its turn, requires the conditions $\tilde{\omega}^2(k_0) \ll m_\pi^2 \approx p_F^2/4$. It is in this sense that proximity to the instability was understood in Ref. 3. It is not important which of the parameters has not yet reached the critical point—the only important thing is the shortfall. Therefore, to investigate precritical effects we can fix the parameters α and ζ_s (setting, for example, $\alpha = 0$ and $\zeta_s = 0.05$) and investigate the effects of proximity to π condensation by varying only the constant g'.[41] We then obtain from (54)

$$\tilde{\omega}^2(k \approx k_0) = m_\pi^2 [2.6(g' - g'_{cr}) + 1.3(k^2 - k_0^2)^2/2k_0^4]. \tag{55}$$

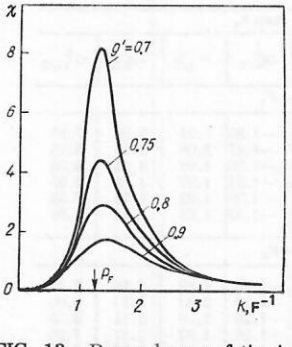

FIG. 13. Dependence of the longitudinal component of the magnetic susceptibility of normal nuclear matter on the momentum transfer k for some values of the spin–isospin constant g'. The calculation was made for $\alpha = 0$, $\zeta_s = 0.05$, $p_F = 1.27\ F^{-1}$ (in this case, $g'_{cr} = 0.637$, $k_0 = 1.33\ F^{-1}$).

Figure 13 demonstrates the dependence of the coefficient $\chi(k)$ of enhancement of the effective field on the proximity to the point of π condensation.

Thus, the first precritical effect is the enhancement of the static effective symmetry field $(\sigma \cdot \mathbf{k})k_\alpha \tau_\beta$ near $k \approx k_0 \approx p_F$ or, in the terminology of Ref. 16, critical opalescence. As we have seen, the influence of this effect on the spectroscopic characteristics of nuclei [the magnetic moments, $B(M1)$, etc.] is, as a rule, small because the result always contains integrals over k in which the enhancement region is weakly represented. Therefore, to find a clearer manifestation of the effect it is natural to turn to nuclear reactions in which one can "adjust" the momentum k transferred to the nucleus. In this case, the source of the external field $V_0(k)$ acting on the nucleus is the weak, electromagnetic, or strong interaction of the incident particle with the nucleus. From the point of view of theory, the first two are preferable, since the interaction with the nucleus is simpler for them. The ideal reaction would be inelastic scattering of neutrinos with excitation of anomalous-parity states, but the experimental possibilities are here very restricted. Electron scattering is rather unsuitable because the magnetic field produced by the electron is transverse and does not excite the longitudinal component V_2 of the effective field, i.e., the component of V that is enhanced near the point of π condensation. In this case the effects of the proximity to the point of π condensation are possible only to the extent of the momentum nonconservation due to the finite size of the nucleus, and they should be sought in the lightest nuclei.[17]

The most suitable reaction appears to be the inelastic scattering of protons with the excitation of anomalous-parity levels. This reaction was proposed by the present authors in Ref. 14 and also by Toki and Weise[18] as a test of the proximity of nuclei to the point of π condensation.

Another effect of proximity to π condensation is the softening of the "pion mode." There is a widespread delusion that softness of the pion mode signifies a strong lowering and collectivization of the low-lying anomalous-parity states,[17,44] and the absence of such a phenomenon experimentally is taken to prove that nuclei are far from the point of π condensation. As we have seen in the previous section, a significant lowering of the individual particle–hole levels occurs only in the immediate proximity of the condensation point, when the frequency determined from (26) satisfies $\omega \approx \tilde{\omega}(k_0)v_F < \Delta\varepsilon_{\lambda\,\min}$. For $\omega > \Delta\varepsilon_{\lambda\,\min}$, the expression (26) becomes invalid and on the right-hand side we must add an imaginary term (for $\omega \ll \varepsilon_F$ and $k \sim p_F$, an estimate gives $\operatorname{Im}\Phi(k,\omega) \simeq \gamma|\omega|/\varepsilon_F$, where $\gamma \sim 1$; see Ref. 27). As a result, all the solutions $\omega_s(k)$ of the dispersion equation (13) become complex. As before, $\operatorname{Re}\omega_s$ is given approximately by the expression (26), and $\operatorname{Im}\omega_s \sim \operatorname{Re}\omega_s$. Solutions of this type do not correspond to stationary states of the system but describe broad resonances in the pion-absorption cross section with frequency $\sim \operatorname{Re}\omega_s$. Since such excitation, like the static pions discussed above, are strongly virtual, it is again necessary to scatter particles on nuclei to produce them.

Leaving aside the question of the choice of a suitable incident particle, Alberico *et al.*[54] calculated the relative cross section of quasielastic scattering by a nucleus, using the expressions for infinite nuclear matter. The cross section of the process is proportional to the imaginary part of the polarization operator $\Pi(\omega,k)$ for the external field produced by the scattered particle; it can be found from the equation

$$\Pi(\omega, k) = \Phi(\omega, k) - \mathcal{F}(\omega, k)\,\Phi(\omega, k)\,\Pi(\omega, k). \tag{56}$$

The source of the imaginary parts is here Φ. After some simple manipulations, we obtain from (56)

$$\operatorname{Im}\Pi(\omega, k) = \frac{\operatorname{Im}\Phi(\omega, k)}{[1+\mathcal{F}(\omega, k)\operatorname{Re}\Phi(\omega, k)]^2 + [\mathcal{F}(\omega, k)\operatorname{Im}\Phi(\omega, k)]^2}. \tag{57}$$

The first term in the denominator of (57) is the expression that determines the dispersion law (22) in the absence of inelastic processes ($\operatorname{Im}\Phi = 0$). The estimate of its ω dependence is $\sim[\omega^2 - \tilde{\omega}_0^2(k)]/\varepsilon_F^2$, where $\tilde{\omega}_0^2(k) \sim v_F^2\tilde{\omega}^2(k)$ [see (26)]. If nuclei are far from the point of π condensation, then $\omega_0 \sim \varepsilon_F$ and for $\omega < \varepsilon_F$ this term is a smooth function of ω and k of order unity, and therefore $\operatorname{Im}\Pi \sim \operatorname{Im}\Phi$, i.e., the correlations in the nucleus do not lead to a singnificant change in the cross section of inelastic processes compared with the approximation of noninteracting particles. In this case, the quasielastic peak at $k \sim p_F$ is at $\omega \sim \varepsilon_F$ and is not clearly expressed. A different situation arises if the nuclei are near π condensation, when $\tilde{\omega}_0$ depends strongly on k and at $k = k_0$ ($\sim p_F$) there is a minimum $\tilde{\omega}_{\min}(k_0) \ll \varepsilon_F$. Then for $\omega \ll \varepsilon_F$, (57) can be approximated by

$$\operatorname{Im}\Pi(\omega, k) \sim \operatorname{Im}\Phi(\omega, k)/[(\omega^2 - \tilde{\omega}_{\min}^2(k_0))^2/\varepsilon_F^4 + \gamma^2\omega^2/\varepsilon_F^2]. \tag{58}$$

It can be seen that $\operatorname{Im}\Pi$ now begins to depend strongly on k: far from k_0 the difference between $\operatorname{Im}\Pi$ and $\operatorname{Im}\Phi$ is again small, but for $k \sim k_0$ the expression (58) has a sharp maximum in the region of $\omega \sim \omega_{\min}(k_0) \ll \varepsilon_F$, i.e.,

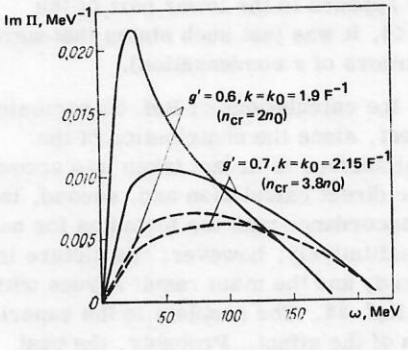

FIG. 14. Imaginary part of the response function of infinite nuclear matter in the spin–isospin channel as a function of the excitation energy at fixed momentum transfer k equal to the critical value k_0 and at normal nuclear density n_0 ($p_F = 1.36$ F^{-1}). The broken curves correspond to a free Fermi gas, and the continuous curves to interacting nucleons. The calculation was made in Ref. 54 for two values of the constant g', for which the corresponding critical densities are indicated. It should be borne in mind that the interaction in Ref. 54 differs somewhat from ours.

the quasielastic peak is shifted to the region of small ω. This shift signifies softening of the pion mode, which, thus, is one of the manifestations of proximity to the point of π condensation.

In Fig. 14, we have plotted graphs of $\mathrm{Im}\,\Pi(\omega, k)$ for $k = k_0$ as calculated in Ref. 54 for two values of g' corresponding to different degrees of proximity to the point of π condensation. The calculation took into account the contribution of virtual production of the Δ isobar, which does not change the qualitative estimates.

Essentially, the same phenomenon was considered by Toki and Weise in Ref. 55, in which they studied the collectivization of anomalous-parity states at large momenta. They calculated the distribution of the transition strengths in an external field of the form $(\sigma \cdot k) \times \exp(ik \cdot r)$ for $k \gtrsim p_F$ in the nucleus ^{208}Pb for the modes with $J^\pi = 0^-, 1^+, 2^-$. The computational scheme was constructed as follows. The equation for the response of the system to an external field of the type of Eq. (28) was solved in a truncated basis of two or three shells, and the remaining particle–hole excitations were taken into account by the introduction of a factor ε_J, the "dimeson function," which renormalizes the pion propagator in accordance with the formulas for an infinite system (analog of the permittivity). The standard calculation in the truncated basis without introduction of the factor ε_J does not lead to appreciable collectivization of the states in the lower part of the spectrum (Fig. 15a). When ε_J is taken into account, the transition strength is transferred from the "distant" transitions to the lower part of the spectrum, and this is more pronounced, the closer the nuclei to the point of π condensation, i.e., the smaller g'. Of course, allowance for the fragmentation of the individual particle–hole states and coupling to the continuum lead in the case of a realistic interaction to merging of the individual lines into a broad resonance, whose center of gravity for $k \sim p_F$ is shifted downward strongly compared to calculations in which there is no softening of the pion mode. It is only very close to the point of π condensation, for $g' = 0.4$,[2] that an individual strongly collectivized state appears in the lower part of the spectrum (in Ref. 44, it was just such states that were regarded as precursors of π condensation).

It is evident that the calculations of Ref. 55 somewhat exaggerate the effect, since the contribution of the states at the Fermi surface is in fact taken into account twice: first, in the direct calculation and, second, in the calculation in accordance with the formulas for an infinite system. Qualitatively, however, the picture is correctly reproduced, and the main result agrees with the conclusions of Ref. 54. The problem is the experimental verification of the effect. Probably, the best "tool" is again a proton, but now polarized, since it is necessary to measure spin-flip cross sections—otherwise the considered resonances will be "drowned" on the background of giant resonances of electric type.

[2] In Ref. 55, approximately the same interaction as in Ref. 25 is used; it differs slightly from the one we use, and therefore corresponds to the different value $g'_{cr} \approx 0.4$.

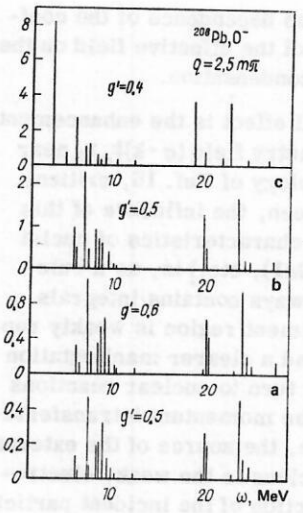

FIG. 15. Probability of excitation (in relative units) of states of the ^{208}Pb nucleus in the external field $(\sigma \cdot k) \exp(ik \cdot r)$ as calculated in Ref. 55. In the lower part of the figure (a) we have the result of the standard calculation in a truncated basis without introduction of the "dimeson function" (the factor $\varepsilon_J = 1$); b), c), and d) are with introduction of the factor ε_J for different values of the constant g'.

6. PRECRITICAL EFFECTS IN THE INELASTIC SCATTERING OF NUCLEONS

A nucleon scattered inelastically by a nucleus produces an external field which, in the general case, is nonlocal and depends on the energy:

$$\hat{V}^0 = \int \mathcal{U}(r_1, r_2, r_3, r_4;\ \varepsilon, \varepsilon', \omega)\, \psi_f^*(r_3)\, \psi_i(r_4)\, dr_3\, dr_4. \qquad (58)$$

Here, ψ_i and ψ_f are the wave functions of the incident and scattered nucleon in the field of the nucleus, and $\mathcal{U}$, which is irreducible in the particle-hole channel, is the set of interaction diagrams of the nucleons. The external symmetry field $\sigma_\alpha \tau_\beta$ in which we are interested arises from the spin–isospin components of $\mathcal{U}$. If the nuclei are near the point of π condensation, the corresponding effective field $V(k)$ at $k \sim k_0$ will be enhanced, which must lead to maxima in the differential cross section of inelastic scattering with the excitation of anomalous-parity states.[14,18] As a rule, in the case of the excitation of low-lying states the contribution of direct processes is dominant, and the distorted-wave Born approximation can be used to describe the reaction.

The distorted-wave Born approximation in the theory of finite Fermi systems. The matrix element M_{0s} for the excitation of the states $|s\rangle$ of an even–even nucleus in the case of inelastic scattering of a nucleon is represented by the diagram

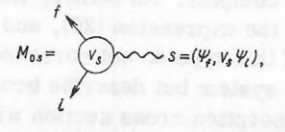

(59)

where v_s is the vertex for production of the state $|s\rangle$. If the state has a particle–hole nature, then v_s is de-

termined by the homogeneous equation

$$v_s(\mathbf{r}_1, \mathbf{r}_2, \varepsilon) = \int \mathcal{U}(\mathbf{r}_1, \mathbf{r}_2, \mathbf{r}_3, \mathbf{r}_4; \varepsilon, \varepsilon', \omega_s) \times G(\mathbf{r}_3, \mathbf{r}_5, \varepsilon' - \omega_s/2) v_s(\mathbf{r}_5, \mathbf{r}_6; \varepsilon') \times G(\mathbf{r}_6, \mathbf{r}_4, \varepsilon' + \omega_s/2)\, d\mathbf{r}_3\, d\mathbf{r}_4\, d\mathbf{r}_5\, d\mathbf{r}_6 \frac{d\varepsilon'}{2\pi i}, \quad (60)$$

where G is the single-particle Green's function. In the theory of finite Fermi systems, the Green's function G is represented as the sum of a quasiparticle part aG^q and a regular part G^R (a is a renormalization factor). Equation (60) can be renormalized in the theory of finite Fermi systems, i.e., it can be formulated in the language of quasiparticles, by means of the standard decomposition of the product GG into two parts:

$$GG = a^2 A + B, \quad (61)$$

where

$$A(\mathbf{r}_1, \mathbf{r}_2, \mathbf{r}_3, \mathbf{r}_4; \varepsilon, \omega) = 2\pi i \delta(\varepsilon - \mu) \int G^q(\mathbf{r}_1, \mathbf{r}_3, \varepsilon' + \omega)\, G^q(\mathbf{r}_4, \mathbf{r}_2, \varepsilon') \frac{d\varepsilon'}{2\pi i}. \quad (62)$$

Here, μ is the chemical potential of the system. Replacing $\mathcal{U}$ by the renormalized amplitude F:

$$F(\varepsilon, \varepsilon', \omega) = a^2 \mathcal{U}(\varepsilon, \varepsilon', \omega) + \int a^2 \mathcal{U}(\varepsilon, \varepsilon_1, \omega) B(\varepsilon_1, \varepsilon_2, \omega) F(\varepsilon_2, \varepsilon_1', \omega) \frac{d\varepsilon_1\, d\varepsilon_2}{(2\pi i)^2}, \quad (63)$$

we obtain from (60)

$$v_s(\varepsilon) = F(\varepsilon, \mu, \omega_s) A(\omega_s) v_s(\mu). \quad (64)$$

The amplitude F in (64) differs from the ordinary amplitude $\mathcal{F}$ in the theory of finite Fermi systems by the dependence on ε and goes over into the latter for $\varepsilon = \mu$. The quantity $v_s(\mu)$ on the right-hand side of (64) already satisfies the usual equation (28) of the theory of finite Fermi systems, this containing the amplitude $\mathcal{F} = F(\mu, \mu)$ for the interaction of quasiparticles at the Fermi surface. Introducing the transition density matrix $\rho^{tr}(\mathbf{r}_1, \mathbf{r}_2) = \langle s | \psi^*(\mathbf{r}_1)\psi(\mathbf{r}_2) | 0 \rangle$ for the excitation of the state $|s\rangle$, which is related to the amplitude $v_s(\mu)$ by

$$\rho^{tr}(\mathbf{r}_1, \mathbf{r}_2) = \int A(\mathbf{r}_1, \mathbf{r}_2, \mathbf{r}_3, \mathbf{r}_4; \omega_s) v_s(\mathbf{r}_3, \mathbf{r}_4; \mu)\, d\mathbf{r}_3\, d\mathbf{r}_4, \quad (65)$$

we rewrite (64) as

$$v_s(\mathbf{r}_1, \mathbf{r}_2; \varepsilon) = \int F(\mathbf{r}_1, \mathbf{r}_2, \mathbf{r}_3, \mathbf{r}_4; \varepsilon, \mu, \omega_s) \rho^{tr}(r_3, r_4)\, dr_3\, dr_4. \quad (66)$$

The expression (66) is very convenient for analysis. In it, the matrix element of the process is represented as the product of the purely structural quantity ρ^{tr}, which characterizes the state $|s\rangle$ and can be completely calculated in the theory of finite Fermi systems, and the amplitude $F(\varepsilon, \mu, \omega_s)$, which contains all the information about the reaction mechanism. The expression (66) is exact. The approximations begin when the amplitude F in (66) is approximated by some simple expression. Neglect of the dependence of F on the frequency ω_s leads to the distorted-wave Born approximation (DWBA). The dependence on ω in F is important when next to the considered state $|s\rangle$ there is another state with the same J^π but not of a particle–hole nature. The explicit separation of this dependence in F leads to the system of equations of the coupled-channel method. We shall now briefly describe the calculations made in Refs. 41 and 56 of the cross sections for the excitation of states of anomalous (negative) parity in the nucleus ^{208}Pb at the height 4–5 MeV. The lowest states of negative parity in this nucleus having a more complicated nature are two-phonon states with energy $\sim\omega_{3^-} + \omega_{2^+} \simeq 6.7$ MeV. Therefore, to analyze the excitation of the considered states we can use the DWBA method.

In the actual calculations, we use F of the form (4), (10), and (11), which contains no velocity dependence:

$$F(\mathbf{r}_1, \mathbf{r}_2, \mathbf{r}_3, \mathbf{r}_4) = F(\mathbf{r}_1, \mathbf{r}_3)\, \delta(\mathbf{r}_1 - \mathbf{r}_2)\, \delta(\mathbf{r}_3 - \mathbf{r}_4).$$

Then $v_s(\mathbf{r}_1, \mathbf{r}_2) = v_s(\mathbf{r}_1)\delta(\mathbf{r}_1 - \mathbf{r}_2)$, etc., as a result of which Eqs. (65) and (66) simplify:

$$v_s(\mathbf{r}, \varepsilon) = \int F(\mathbf{r}, \mathbf{r}'; \varepsilon, \mu, \omega_s) \rho^{tr}(\mathbf{r}')\, d\mathbf{r}', \quad (67)$$

where

$$\rho^{tr}(\mathbf{r}) = \int A(\mathbf{r}, \mathbf{r}'; \omega_s) v_s(\mathbf{r}', \mu)\, d\mathbf{r}'. \quad (68)$$

Qualitative analysis. In the qualitative analysis of the effect, it is convenient to calculate $v_s(\mu)$ using Eqs. (40)–(42) with separated transition $1 \to 2$, which makes the dominant contribution to the transition density ρ^{tr}. Substituting A_0 explicitly in (41) and going over to the momentum representation, we obtain (without writing out explicitly the obvious summation over the magnetic quantum numbers)

$$v_s(k) = \frac{1}{\omega_s - \omega_{12}} \int \Gamma'(\mathbf{k}, \mathbf{k}'; \omega_s) \chi_{12}(\mathbf{k}') \chi_{12}^*(\mathbf{k}'') v_s(\mathbf{k}'') \frac{d\mathbf{k}'\, d\mathbf{k}''}{(2\pi)^6}, \quad (69)$$

where

$$\chi_{12}(\mathbf{k}) = \int \exp(i\mathbf{k}\mathbf{r})\, \varphi_1^*(\mathbf{r})\, \varphi_2(\mathbf{r})\, d\mathbf{r}.$$

Now, since we are interested in the region $k \sim p_F$, we can use the approximation $\Gamma'(\mathbf{k}, \mathbf{k}') = (2\pi)^3 \delta(\mathbf{k} - \mathbf{k}')\Gamma(\mathbf{k})$, where $\Gamma(\mathbf{k})$ is given by Eqs. (13)–(17) for infinite nuclear matter. Ignoring the term $dA'/d\omega$ in the normalization condition (29) (this is justified for noncollective states) and separating the angular variables by means of the formulas in the Appendix, we obtain

$$v_J^L(k) = \frac{1}{\sqrt{2J+1}} \sum_{L'} i^{L'-L} \Gamma_J^{LL'}(k) \chi_{12}^{L'}(k) \langle j_1 l_1 \| T_{JL'1} \| j_2 l_2 \rangle. \quad (70)$$

Here, $L, L' = J \pm 1$,

$$\chi_{12}^L(k) = \int j_L(kr) R_1(r) R_2(r) r^2\, dr, \quad (71)$$

$$\Gamma_J^{LL'}(k) = C_0 \{ [G(k) + G'(k) \tau_1 \tau_2] \delta_{LL'} + C_J^{LL'} T(k) k^2 \tau_1 \tau_2 \}, \quad (71')$$

where the coefficients $C_J^{LL'}$ are given by (A6), and $G(k)$, $G'(k)$, and $T(k)$ by Eqs. (16) and (17). The denominators in $T(k)$ and the longitudinal component $V_2(k)$ of the effective field [Eq. (20)] are the same, and therefore near the point of π condensation when $k \sim k_0$ the amplitude $T(k)$, and with it $v_J^L(k)$, has the same amplification as $V_2(k)$ (see Fig. 13).

Rewriting Eqs. (67) and (68) in the momentum representation and using the circumstance that for $k \sim p_F$ we have $A(\mathbf{k}, \mathbf{k}') \simeq -C_0^{-1} \Phi(k) \delta(\mathbf{k} - \mathbf{k}')$, $F(\mathbf{k}, \mathbf{k}'; \varepsilon, \mu) \sim F(k; \varepsilon, \mu) \delta(\mathbf{k} - \mathbf{k}')$, where $\Phi(k)$ and $F(k; \varepsilon, \mu)$ are smooth functions of k, we arrive at the conclusion that the maximum at $k \sim k_0$ in $v_s(\mu)$ is also transferred to $v_s(\varepsilon)$. This effect must lead to the appearance of a characteristic maximum in the inelastic-scattering cross section at angles corresponding to $k \sim k_0$ [at least in the plane-wave Born approximation (PWBA)]. As we shall see, the introduction of distorted waves

significantly complicates the picture, but at proton energies $E_p \gtrsim 100$ MeV the effect must survive.

Exact calculation of the transition density. The main uncertainties in the calculation of the reaction cross section on the basis of Eqs. (59), (65), and (66) are due to the fact that the energy dependence of the amplitude $F(\varepsilon, \mu)$ is not well known. At the same time, the entire considered effect in Eq. (66) is contained in the transition density ρ^{tr}, which can be calculated fairly reliably by the methods of the theory of finite Fermi systems. It is therefore natural to divide the problem into two stages. The first stage, the structural calculation of ρ^{tr} for a given form of $\mathcal{F}$, can be done exactly in the coordinate representation by means of the method described above. This part of the calculation was carried out in Ref. 41 for three anomalous-parity states in ^{208}Pb(2_1^-, 4_1^-, and 6_1^-) and with several values of the constants that measure the proximity to the point of π condensation. The results were tabulated in a form convenient for use in calculations of the reaction cross sections by the DWBA method or by Glauber's method, and also for the calculation of the form factors of inelastic electron scattering. In Fig. 16, we give the amplitude $v_s(k, \mu)$ for production of the 0^- state in ^{208}Pb as a function of k obtained as a result of the exact solution. It can be seen that in the exact solution for v_s the effect is expressed as clearly as in the approximate solution (see Fig. 13). In Fig. 17 we show the Fourier transform of $\rho^{tr}(k)$, which corresponds to the transition density. One can clearly see a maximum at $k \sim k_0$. Finally, Fig. 18 demonstrates the effect in the Born differential cross section calculated in the approximation $F(\varepsilon, \mu) = F(\mu, \mu)\mathcal{F}$ [with $v_s(\varepsilon) = v_s(\mu)$].

Calculation of cross sections by the DWBA *method*. The calculation of the matrix element (58) by means of Eq. (66) includes two new elements: the amplitude $F(\varepsilon, \mu)$ of the interaction of the incident proton with the nucleons of the nucleus and the optical potential of the nucleus, which is needed to calculate the functions Ψ_i and Ψ_f. The energy dependence of the spin components of F is not well known, and our main hope here is that their dependence on the momentum transfer k at $k \sim 1$–2 F^{-1} is rather weak and cannot smear the k peak in the Fourier components of the transition density at $k = k_0$ (see Fig. 17).

To investigate the part played by the distorted waves, an attempt was made in Ref. 56 to calculate the cross

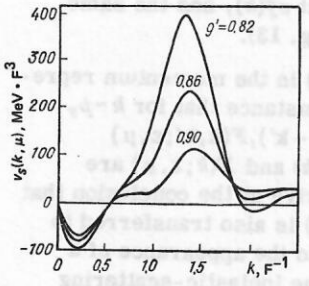

FIG. 16. Amplitude $v_s(k, \mu)$ for production of 0^- states in ^{208}Pb as a function of k, calculated for different values of the constant g'.

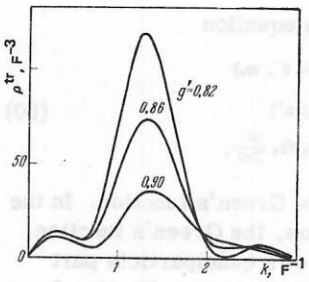

FIG. 17. Transition density $\rho^{tr}(k)$ for the 0^- states in ^{208}Pb as a function of k for different values of the constant g'.

sections at different proton energies E_p with $F(\varepsilon, \mu)$ in (66) replaced by the amplitude $\mathcal{F} = F(\mu, \mu)$ of quasiparticle interaction at the Fermi surface.

The differential cross sections were calculated in the framework of the DWBA method by means of the program DWBAX, which was specially written for this purpose. This program makes it possible to describe elastic and inelastic scattering of protons by nuclei at energies $E_p < 200$ MeV in an optical potential of standard form (see, for example, Ref. 58):

$$U = V_C(r) - Vf(r; R_v, a_v) + (V_{ls} + iW_{ls})\frac{2}{r}\frac{d}{dr}f(r; R_{ls}, a_{ls})(\sigma l) + i\left(-W_v + 4W_s a_s \frac{d}{dr}\right) f(r; R_w, a_w), \quad (72)$$

where V_C is the Coulomb potential of a uniformly charged sphere with total charge Ze and radius $R_c = r_{0c}A^{1/3}$, V is the depth of the real part of the central potential, W_v and W_s are the intensities of the volume and surface imaginary parts of the optical potential, and V_{ls} and W_{ls} are the parameters of the real and imaginary parts of the spin–orbit potential. The radial dependences of the functions f are specified in the Woods–Saxon form, $f(r; R_i, a_i) = \{1 + \exp[(r - R_i)/a_i]\}^{-1}$ with radius $R_i = r_{0i}A^{1/3}$ and diffuseness a_i ($i = v, s, ls$).

Successive inclusion of the real and imaginary parts of the optical potential U showed that the modification of the momentum distribution is mainly due to ReU. The peak at $k = k_0$ in the Born cross section is strongly smeared up to $E_p \lesssim 60$ MeV. The effect of the distortions decreases with increasing E_p and becomes slight when $E_p \gtrsim 100$ MeV. The imaginary part ImU of the optical potential has little influence on the profile of

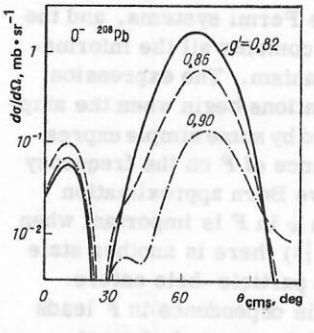

FIG. 18. Born cross section for inelastic scattering of protons with excitation of 0^- states in ^{208}Pb, calculated under the assumption $F(\varepsilon, \mu) = F(\mu, \mu) = \mathcal{F}$ for different values of the constant g'.

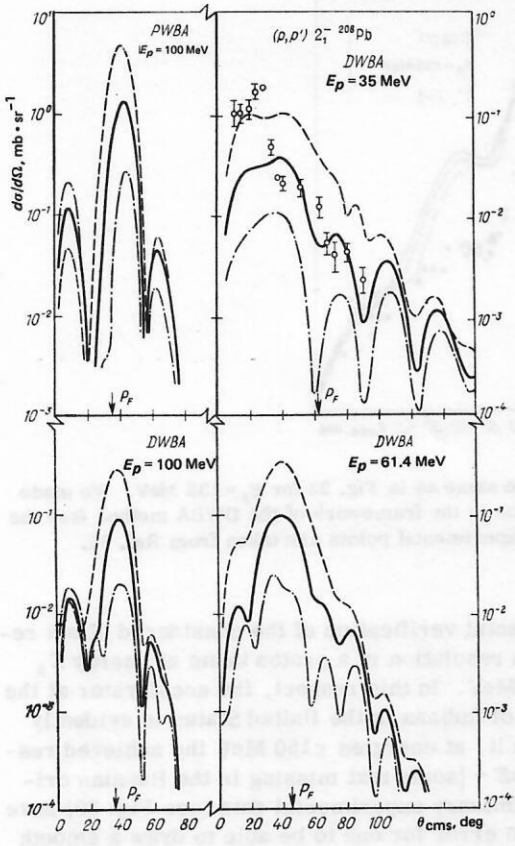

FIG. 19. Cross sections for inelastic scattering of protons with excitation of a 2_1^- state in ^{208}Pb, calculated with the transition densities from Ref. 41. For a description of optical potential, see the text. The experimental data for $E_p = 35$ MeV are taken from Ref. 57.

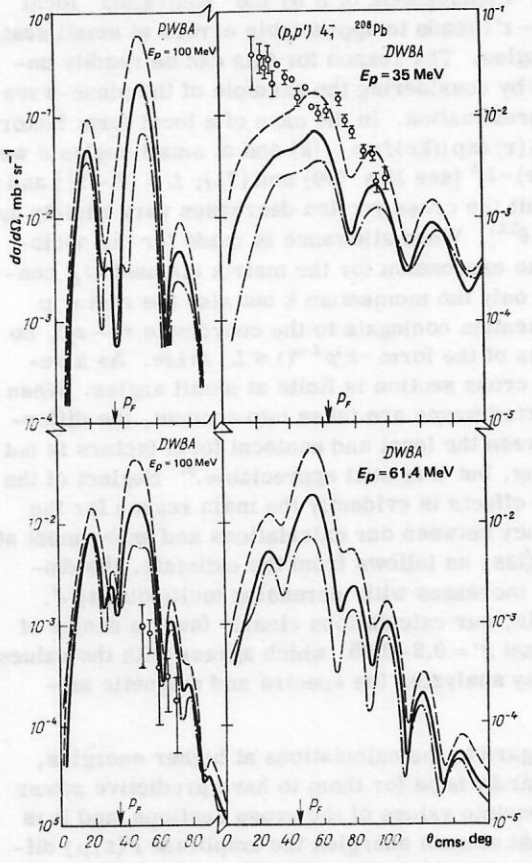

FIG. 20. The same as in Fig. 19 for the 4_1^- state in ^{208}Pb. For $E_p = 100$ MeV, the experimental data from Ref. 62 are given.

the cross section, but strongly (by up to an order) reduces its magnitude. This effect persists at higher energies.

The results of calculation of the excitation cross sections of the levels 2_1^-, 4_1^-, and 6_1^- in ^{208}Pb for 35, 60, and 100 MeV are given in Figs. 19–21. The parameters of the optical potential for the energy 35 MeV were taken from Ref. 58, and for the energies 60 and 100 MeV from Ref. 59. It can be seen that at $E_p = 35$ MeV the distorted waves smear the effect so much that virtually nothing remains of the peak at $k = k_0$. At $E_p = 60$ MeV, the peak survives, though it is rather broad, while at $E_p = 100$ MeV the cross section has a profile near that of the Born cross section.

We now consider the problem of comparing calculations with the experiment of Ref. 57 at $E_p = 35$ MeV. At this energy, the replacement of the amplitude F in (66) by $\mathscr{F}$ appears reasonable. Indeed, F is some mean value between the amplitude $\mathscr{F} = F(\mu, \mu)$ in the theory of finite Fermi systems and the vacuum amplitude $F^{vac}(E_p, \mu)$, but at such energies they differ little.[60] More important is evidently a different defect of our amplitude—the neglect of the nonlocality of the exchange terms (for example, $\tilde{\mathscr{F}}_\pi$). Allowance for the nonlocality of F in Eqs. (65) and (66) leads to a nonlocal form factor

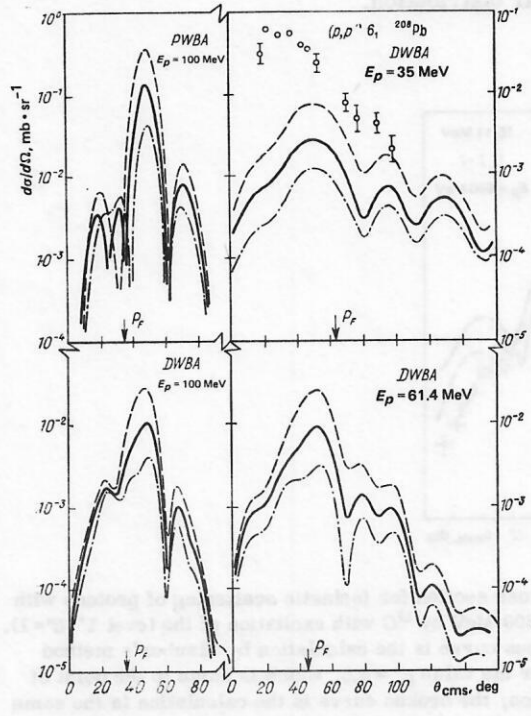

FIG. 21. The same as in Fig. 19 for the 6_1^- state in ^{208}Pb.

$v_J(\mathbf{r},\mathbf{r}')$. Replacement of it by the "equivalent" local $v_J(\mathbf{r})\delta(\mathbf{r}-\mathbf{r}')$ leads to appreciable errors at small scattering angles. The reason for this can be readily understood by considering the example of the plane-wave Born approximation. In the case of a local form factor, $M_{if}=\int v_J(\mathbf{r})\exp(i\mathbf{kr})d\mathbf{r}=v_J(\mathbf{k})$ and at small angles θ we have $v_J(k)\sim k^L$ [see Eqs. (70) and (71); $L=|J-1|$] and as a result the cross section decreases very rapidly as $\theta\to 0$ (as θ^{2L}). When allowance is made for the nonlocality, the expression for the matrix element M_{if} contains not only the momentum k but also the vector p (the momentum conjugate to the coordinate $\mathbf{r}_1-\mathbf{r}_2$), so that terms of the form $\sim k^{\lambda}p^{L-\lambda}(\lambda\leq L)$ arise. As a result, the cross section is finite at small angles. When the distorted waves are taken into account, the difference between the local and nonlocal form factors is not so striking, but it is still appreciable.[57] Neglect of the exchange effects is evidently the main reason for the discrepancy between our calculations and experiment at small angles; as follows from the estimate, the discrepancy increases with increasing multipolarity J. As a whole, our calculations clearly favor a choice of the constant $g'=0.8-0.85$, which agrees with the values obtained by analyzing the spectra and magnetic moments.

With regard to the calculations at higher energies, one can hardly hope for them to have predictive power for the absolute values of the cross sections, and it is evident that at such energies the amplitude $F(\varepsilon,\mu)$ differs appreciably from the interaction $\mathcal{F}$ we have used. For $E_p\gtrsim 100$ MeV, it would be more realistic to make calculations with the vacuum amplitude $F^{\text{vac}}(E_p,\mu)$, but unfortunately such calculations have not yet been made. Our calculations indicate only that a qualitative effect at such energies must be noticeable, although the momentum dependence of $F^{\text{vac}}(E_p,\mu)$ may somewhat modify the angular distribution.

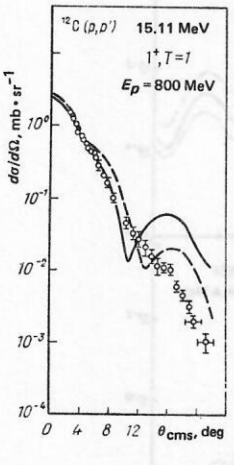

FIG. 22. Cross section for inelastic scattering of protons with energy $E_p=800$ MeV by ^{12}C with excitation of the level 1^+ ($T=1$). The continuous curve is the calculation by Glauber's method in Ref. 63 for the value $g'=0.5$, which is close to the point of π condensation; the broken curve is the calculation in the same paper without allowance for the effects that lead to "critical opalescence." The experimental points are taken from Ref. 64.

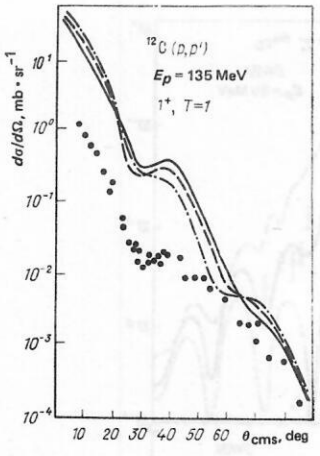

FIG. 23. The same as in Fig. 22 for $E_p=135$ MeV. We made the calculation in the framework of the DWBA method (see the text). The experimental points are taken from Ref. 65.

Experimental verification of the considered effect requires high resolution in a proton beam at energy $E_p=100-200$ MeV. In this respect, the accelerator at the University of Indiana in the United States is evidently optimal; in it, at energies $\lesssim 150$ MeV the achieved resolution is $\Delta E\sim$ [some text missing in the Russian original] preliminary experimental data (see Fig. 20) have too large an error for one to be able to draw a smooth curve. The fact that the absolute values of the experimental cross section are somewhat below the results of our calculations (and for all values of g') indicates that at $E_p\sim 100$ MeV the amplitude $F(E_p,\mu)$ is two or three times smaller than $F(\mu,\mu)$.

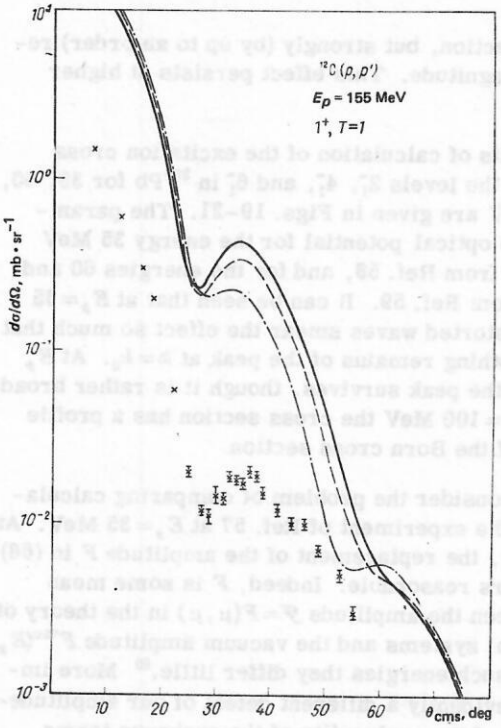

FIG. 24. The same as in Fig. 23 for $E_p=155$ MeV. The experimental points are from Ref. 66.

Recently, the level $1_2^+(T=1)$ in ^{12}C has attracted much interest. It was largely stimulated by Ref. 17, in which the appreciable discrepancy between the experimental form factor of inelastic (e,e') scattering and the results of shell calculations in the region $k \approx 1.5-2$ F^{-1} was interpreted as a precritical effect (critical opalescence). In Ref. 63, Toki and Weise calculated the differential cross section for excitation of the same level by fast ($E_p = 800$ MeV) protons. In the calculation of the cross section, they used Glauber's method. This method is effectively close to the PWBA, and the calculations in Ref. 63, like ours in the DWBA, include the use of a factor that is not well known—the NN forward scattering amplitude, whose spin components have not been well studied. It is therefore no surprise that the recent experiment[64] does not agree with the prediction of Ref. 63 in the absolute magnitude of the cross section (Fig. 22). More important is the fact that the profile of the theoretical curve of the differential cross section with the characteristic peak at angles corresponding to the momentum transfer $k \approx 1.5$ F^{-1}—the "precursor" of pion condensation—is not reproduced in the experiment. It is interesting that at lower energies $E_p = 135$ MeV (Ref. 65) and $E_p = 155$ MeV (Ref. 66) this peak does become noticeable (Figs. 23 and 24, respectively). Our calculations (see Fig. 24) reproduce rather well the profile of the curve, but, as in the case of the 4_1^- state in ^{208}Pb, lead to absolute values of the cross section which are too large. The main reason for this is evidently the same.

Irrespective of the agreement or disagreement of particular calculations for ^{12}C with the experimental data, it should be noted that this nucleus is too light for any reliable application of the theory of finite Fermi systems or similar many-body methods, so that, in our view, the study of this nucleus can hardly cast light on the question of the proximity of nuclei to the point of π condensation. Much more promising in this respect

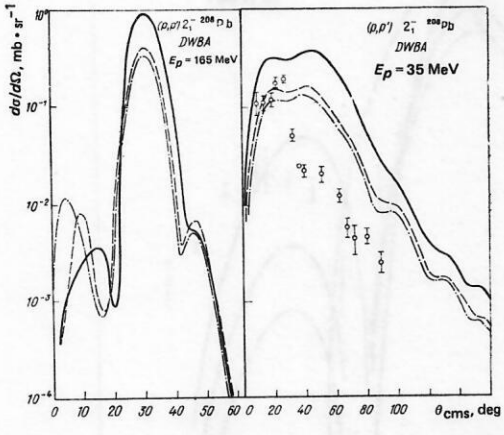

FIG. 25. Cross sections for inelastic scattering of protons with $E_p = 165$ MeV (a) and $E_p = 35$ MeV (b) by ^{208}Pb, calculated for different "equivalent" sets of parameters corresponding to the same degree of proximity to the point of π condensation [corresponding to the same value of $\tilde{\omega}^2(k_0)$ in (54)]. The chain curve corresponds to the "standard" set $\alpha = 0$, $\zeta_s = 0.05$, $g' = 0.85$; the broken curve, to $\alpha = 0$, $\zeta_s = 0.1$, $g' = 0.55$; the continuous curve, to $\alpha = 0.3$, $\zeta_s = 0.05$, $g' = 0.592$.

are experiments on the scattering of fast ($E_p \gtrsim 100$ MeV) protons with the excitation of anomalous-parity states in ^{208}Pb and other heavy nuclei; such experiments have already been started using the accelerator at the University of Indiana.

To conclude this section, we shall demonstrate that although the considered enhancement of the effective spin–isospin field near the point of π condensation does depend strongly on the parameters of the amplitude $\mathcal{F}$, this dependence is greatly weakened if the value of $\tilde{\omega}^2(k_0)$ in (54) is fixed. For this, calculations were made for three sets of the parameters (α, g', ζ_s) corresponding to the same $\tilde{\omega}^2(k_0)$ (Fig. 25). It can be seen that for all three sets the considered precritical effect is, at least qualitatively, reproduced, so that it really is a result of the small value of $\tilde{\omega}^2(k_0)$, which indicates that nuclei are close to the point of π condensation.

7. SEARCH FOR EFFECTS OF PROXIMITY TO THE POINT OF π CONDENSATION IN THE MAGNETIC SCATTERING OF ELECTRONS

At the present time, electron scattering is the "cleanest" tool for studying the structure of nuclei. The inelastic scattering of an electron with excitation of the state $|s\rangle$ is determined by the diagram in Fig. 26. In contrast to the case of proton scattering, the form of the "external field" exerted by the scattered electron on the nucleus ($\hat{V}_0 = \int_N \mathbf{A}_{em}$) does not contain unknown factors, which makes it possible to obtain reliable information on the structure of the transition density of the excited state. Moreover, up to almost the heaviest nuclei one does not have to employ a cumbersome method such as the DWBA in an approximate calculation of the cross sections but can use the eikonal approximation, which reduces to the Born approximation by the simple replacement of the electron momentum p by $p_{eff} = p(1 + 3/2\, Ze^2/RE_e)$, where R is the radius of the nucleus, Z is its charge, and E_e is the electron energy. In the case of inelastic magnetic scattering, the differential cross section in the ultrarelativistic limit ($E_e \gg m_e, \omega_s$) in the Born approximation has the form

$$\frac{d\sigma}{d\Omega} = \sigma_M \left(1/2 + \tan^2\frac{\theta}{2}\right) F_M^2(k). \tag{73}$$

Here, σ_M is the Mott cross section,

$$\sigma_M = \left(\frac{Ze^2}{2E_e}\right)^2 \frac{\cos^2\theta/2}{\sin^4\theta/2}, \tag{74}$$

and $F_M(k)$ is the magnetic form factor, which for $0^+ \to J^\pi$ transitions without allowance for the convection current has the form

$$F_M(k) = \frac{\sqrt{4\pi}}{Z}\frac{k}{2M}\sum_{\tau=p,\,n}\tilde{\gamma}_\tau\left[\sqrt{J+1}\,\rho_{J,J-1}^{tr(\tau)}(k) - \sqrt{J}\,\rho_{J,J+1}^{tr(\tau)}(k)\right], \tag{75}$$

where k is the momentum transfer, $\gamma_p = \gamma_p - (\gamma_p - \gamma_n)\zeta_s$, $\gamma_n = \gamma_n + (\gamma_p - \gamma_n)\zeta_s$, and $\rho_{J,L}(k)$ is the Fourier transform of the transition density $\rho_{J,L}^{tr}(r)$:

$$\rho_{J,L}^{tr}(k) = \int \rho_{J,L}^{tr}(r)\, j_L(kr)\, r^2\, dr. \tag{76}$$

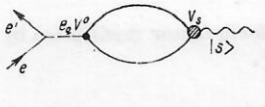

FIG. 26. Diagram of inelastic electron scattering.

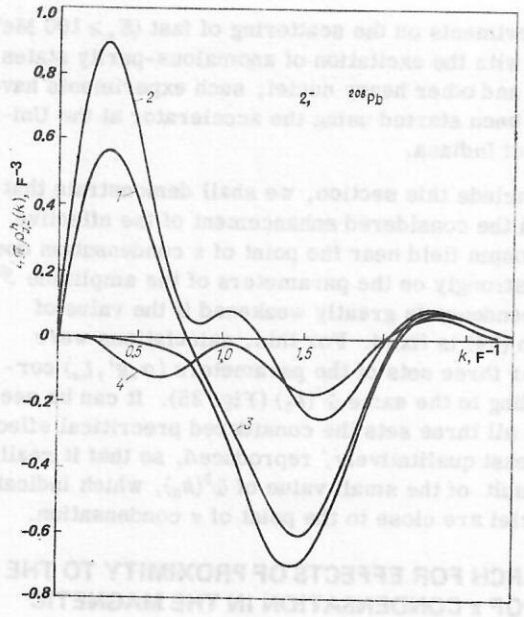

FIG. 27. Fourier transforms of the individual components $\rho^{tr}_{J,L}$, the transition density of the 2^-_1 state in ^{208}Pb, calculated for different g'. Curves 1 and 2 show $\rho^{tr}_{2,1}(k)$ for $g'=0.8$ and $g'=1.0$, respectively; 3 and 4 are the same for $\rho^{tr}_{2,3}(k)$.

The possibilities of using electron scattering to investigate the effects of proximity to the point of π condensation are restricted by the circumstance that the spin component of the nucleon current has only a transverse component ($\sim[\sigma\times\mathbf{k}]$). Therefore, in electron scattering the longitudinal modes of the effective field, which include the "pion" mode enhanced near the point of π condensation, are excited only by virtue of the momentum nonconservation due to the finiteness of the nucleus. Thus, in inelastic magnetic scattering by a heavy nucleus proximity to the point of π condensation need not be clearly manifested. This fact is demonstrated by the example of the level 2^-_1 in ^{208}Pb. Figure 27 shows the neutron components of $\rho^{tr}_{2,L}(k)$, $L=1,3$, calculated for the value $g'=0.8$, which is close to the point of π condensation, and for $g'=1$. It can be seen

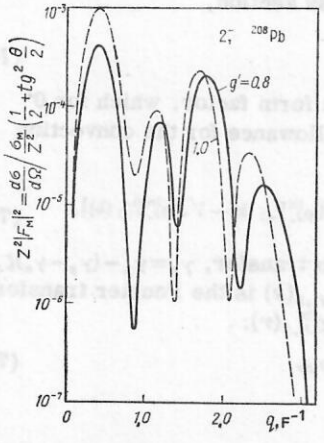

FIG. 28. Square of the magnetic form factor (multiplied by Z^2) of the 2^-_1 state in ^{208}Pb for real g'.

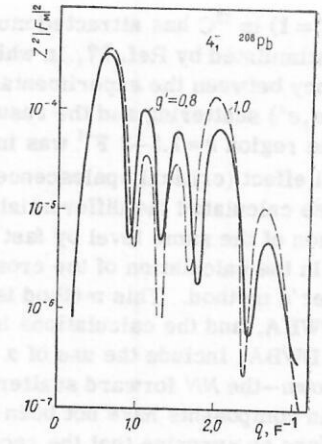

FIG. 29. The same as in Fig. 28 for the 4^-_1 state in ^{208}Pb.

that each of the components is enhanced near $k\approx 1.5$ F^{-1} appreciably for $g'=0.8$ and much less for $g'=1$. But when we consider the total result, the two $\rho^{tr}_{J,L}$ components, which occur in (75) with opposite signs, almost cancel each other at the maximum, so that as a result the form factors in the cases $g'=0.8$ and $g'=1$ are nearly equal (Fig. 28). The situation is the same in the case of the state 4^-_1 in ^{208}Pb (Fig. 29).

The almost complete canceling of the effect in heavy nuclei forces us to light nuclei, in which the canceling may be reduced by the effects of momentum nonconservation. In Ref. 17, the excitation by electrons of the 1^+ level in ^{12}C was considered. The well-known anomaly of the form factor in the region $k\sim 2$ F^{-1} (a discrepancy by almost an order of magnitude between the experimental form factor and the theoretical one found

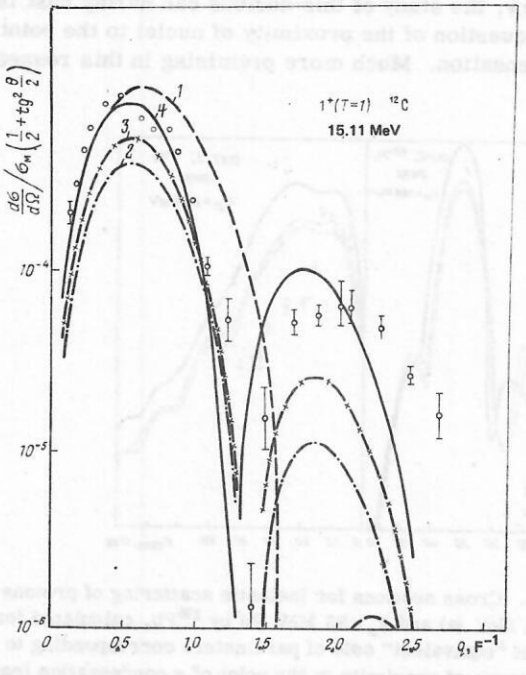

FIG. 30. Square of the magnetic form factor of the state 1^+ (15.1 MeV) in ^{12}C. Curve 1 is the calculation in the shell model without interaction. Curve 2 corresponds to $g'=0.8$, curve 3 to $g'=0.6$, and curve 4 to $g'=0.5$.

on the basis of shell calculations) was discussed. This discrepancy can be eliminated if it is assumed that the nucleus ^{12}C is very close to the point of π condensation for the 1^+ mode in this nucleus. In Ref. 17, an interaction somewhat different from ours was used together with an oscillator single-particle potential. We made a similar calculation with our interaction and with a Woods–Saxon potential. The results are shown in Fig. 30. It can be seen that the calculation with the realistic value $g' = 0.8$ (curve 2) leads to a maximum at the necessary place, but its value is much less than in the experiment. Even when the constant g' is reduced to 0.6 (curve 3) the enhancement effect is very slight. The necessary enhancement is achieved only very close to the point of π condensation: Curve 4 corresponds to $g' = 0.5$, whereas $g'_{cr} = 0.48$ for the 1^+ mode in ^{12}C. This result agrees with the results of the calculations in Ref. 17. However, the conclusion in Ref. 17 that critical opalescence has been discovered in ^{12}C does not convince us for the following reasons. First, although there are no particular reasons for assuming that the constant g' in ^{12}C is the same as in heavy nuclei, such a large change, from $g' = 0.8$–0.85 in ^{208}Pb to $g' \simeq 0.5$ in ^{12}C, appears improbable. But the assumption that in heavy nuclei too $g' \simeq 0.5$ would mean that in them π condensation has already occurred, which contradicts the entire general picture described above. Second, in the nucleus ^{12}C itself the choice $g' \simeq 0.5$ means either that condensation of the 0^- mode has already occurred or such a proximity to π condensation that in any case the use of the "self-consistent field" approximation as used by us and in Ref. 17 is impossible (see, for example, Ref. 67). Finally, there have been fairly successful attempts to eliminate the anomaly of the form factor by more traditional means.[68,69]

Thus, electron magnetic scattering is hardly suitable for detecting or demonstrating the effects of proximity to the point of π condensation. However, bearing in mind the reliability of the theoretical description of the interaction of electrons with nuclei and the high accuracy achieved in recent years in such experiments, it can be hoped that data on the excitation of anomalous-parity levels by electrons will permit better determination of the form of the amplitude $\mathcal{F}$ at large momentum transfers. The high resolution ($\lesssim$30 keV) (Ref. 70) achieved in recent years for electron beams of high energies (up to 500 MeV) makes it possible to obtain

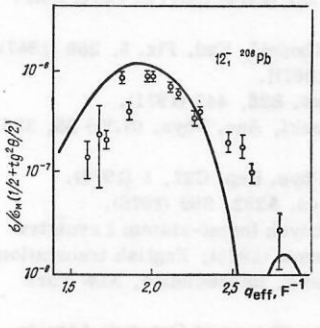

FIG. 31. Square of the magnetic form factor of the 12_1^- state in ^{208}Pb. The calculation was made for the interaction parameters $\alpha = 0$, $\zeta_s = 0.05$, $g' = 0.8$, $g = 0.3$.

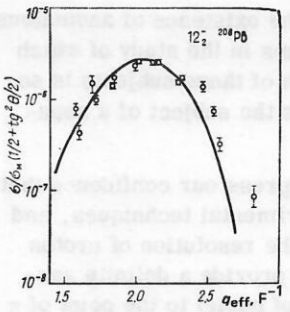

FIG. 32. The same as in Fig. 31 for the 12_2^- state in ^{208}Pb.

the inelastic form factors of individual states even in ^{208}Pb. Thus, the form factors of the states 12_1^- and 12_2^- in this nucleus were measured in Ref. 71. They are shown in Figs. 31 and 32, respectively, together with the results of our calculations. It can be seen that the calculations agree very well with the experiment, which indicates once more that our interaction is realistic and that its parameters have been correctly found in a first approximation.

8. CONCLUSIONS

This review has been devoted to the problem of π condensation in nuclei. We posed three questions.

1. Is there a π condensate in nuclei?

The answer to this question is probably negative. This is based on the absence of the effects predicted if a condensate does exist: anomalies in elastic electron scattering, the "doubling of levels," and an appreciable single-nucleon width of π atoms.

2. Are nuclei close to the point of π condensation?

The answer to this question is apparently positive (by proximity, we understand significant softening of the "pion mode"). Our answer is based mainly on analysis of the spectroscopic characteristics of nuclei (the spectra of the anomalous-parity states and the M1 characteristics), but it is also confirmed by some data on the inelastic scattering of protons and electrons.

3. What effects must result from the proximity of nuclei to the point of π condensate?

The main effect predicted in this connection is the presence of a characteristic maximum in the differential cross section for inelastic scattering of fast ($E_p \gtrsim 100$ MeV) protons by nuclei with the excitation of anomalous-parity states. Such an experiment in heavy nuclei requires a high resolution of the proton beam and is at present possible in only a few accelerators. The commencement of such experiments using the accelerator of the University of Indiana has been announced.

In this review, we have not considered a very large and interesting field—the interaction of slow pions with nuclei, which is intimately related to the problem of the proximity of nuclei to the point of π condensation; nor have we considered interesting questions such as the manifestations of such proximity in collisions of

heavy nuclei, the problem of the existence of anomalous nuclei, and some other problems in the study of which we have not participated. Each of these subjects is so extensive that it could serve as the subject of a separate review.

Finally, we should like to express our confidence that the rapid development of experimental techniques, and above all the improvement in the resolution of proton and electron beams, will soon provide a definite answer concerning the proximity of nuclei to the point of π condensation. Whatever the answer, the corresponding experiments will greatly deepen our understanding of many aspects of the problem of nuclear structure and the interaction of nuclei with particles of medium energies.

APPENDIX

Here, we give the formulas for expanding the amplitude $\mathcal{F}$ and the propagator A in Eqs. (1), (2), and (28) with respect to the spin–angle tensors:

$$T_{JLSM}(\mathbf{n},\sigma)=\sum_m C^{JM}_{LM-mSm}Y_{LM-m}(\mathbf{n})[\sigma_m]^s. \tag{A.1}$$

Here, $C^{JM}_{Lm_1Sm_2}$ is a Clebsch–Gordan coefficient, $Y_{Lm}(\mathbf{n})$ is a spherical function, $[\sigma_m]^0=\delta_{m0}$, and $[\sigma_m]^1=\sigma_m$. For the case of anomalous parity ($S=1$)

$$\mathcal{F}(\mathbf{r}_1,\mathbf{r}_2)=\sum_{JL_1L_2M}\mathcal{F}^{L_1L_2}_J(r_1,r_2)T^+_{JL_11M}(\mathbf{n}_1,\sigma_1)T_{JL_21M}(\mathbf{n}_2,\sigma_2). \tag{A.2}$$

For $\mathcal{F}$ defined by Eqs. (4), (5), and (10) we have

$$\mathcal{F}^{L_1L_2}_J(r_1,r_2)=\mathcal{F}^{L_1L_2}_{0J}(r_1,r_2)+\mathcal{F}^{L_1L_2}_{\pi J}(r_1,r_2), \tag{A.3}$$

where

$$\mathcal{F}^{L_1L_2}_{0J}(r_1,r_2)=C_0\frac{\delta(r_1-r_2)}{r_1r_2}(g+g'\tau_1\tau_2)\delta_{L_1L_2}, \tag{A.4}$$

$$\mathcal{F}^{L_1L_2}_{\pi J}(r_1,r_2)=-1{,}15C_0(1-2\zeta_s)^2C^{L_1L_2}_Jf^{L_1L_2}_\pi(r_1,r_2)\tau_1\cdot\tau_2. \tag{A.5}$$

Here, the angular coefficients $C^{L_1L_2}_J$ are

$$C^{J-1,J-1}_J=J/(2J+1),\quad C^{J+1,J+1}_J=(J+1)/(2J+1),$$
$$C^{J-1,J+1}_J=C^{J+1,J-1}_J=-\sqrt{J(J+1)}/(2J+1). \tag{A.6}$$

and $f^{L_1L_2}_\pi$ (for $-1.4<\alpha<0.7$) is determined by the expression

$$f^{L_1L_2}_\pi(r_1,r_2)=\delta(r_1-r_2)/(r_1r_2)-(2/\sqrt{r_1r_2})\cdot\mathrm{Re}\{ab^2[K_{L_1+\frac12}(br_1)\times I_{L_2+\frac12}(br_2)\theta(r_1-r_2)+K_{L_2+\frac12}(br_2)I_{L_1+\frac12}(br_1)\theta(r_2-r_1)\}, \tag{A.7}$$

where $I_\nu(z)$ are modified Bessel functions, and $K_\nu(z)$ are MacDonald functions. The constants a and b depend on the parameters of the amplitude $\mathcal{F}_\pi$:

$$a=\frac{1-b_0}{2\sqrt{\frac14B^2-0.23}},\quad b=\frac{m_\pi^2}{0.23}b_0, \tag{A.8}$$

where

$$b_0=\frac12B-\sqrt{\frac14B^2-0.23},\quad B=1+0.23-0.9(1-\alpha). \tag{A.9}$$

Similarly, we have the definitions

$$A^{LL'(\tau\tau')}_J(r_1,r_2,\omega)=\sum_{lj\bar l'j'}\langle jl\|T_{JL1}\|j'l'\rangle\times\langle jl\|T_{JL'1}\|j'l'\rangle/(2J+1)\{\sum_n k_{nlj\tau}R_{nlj\tau}(r_1)\times R_{nlj\tau}(r_2)G^{\tau'}_{lj'j'}(r_1,r_2;\varepsilon_{nlj\tau}-\omega)+\sum_{n'}k_{n'l'j'\tau'}\times G^\tau_{lj}(r_1,r_2;\varepsilon_{n'l'j'\tau'}+\omega)R_{n'l'j'\tau'}(r_1)R_{n'l'j'\tau'}(r_2)\}. \tag{A.10}$$

Here, $k_{nlj\tau}$ are the population factors of the single-particle level with the quantum numbers $nlj\tau$, and $R_{nlj\tau}$ is the radial wave function of this level; $G^\tau_{lj}(r_1,r_2;\varepsilon)$ is the Green's function of the radial Schrödinger equation, and $\langle jl\|T_{JL_1}\|j'l'\rangle$ is the reduced matrix element of the spin–angle tensor. The method of calculating $G^\tau_{lj}(r_1,r_2;\varepsilon)$ in the coordinate representation is described in Refs. 20 and 29.

[1]A. B. Migdal, Zh. Eksp. Teor. Fiz. **61**, 2209 (1971); **63**, 1993 (1972) [Sov. Phys. JETP **34**, 1184 (1972); **36**, 1052 (1973)]; Nucl. Phys. **A210**, 421 (1973).
[2]R. F. Sawyer, Phys. Rev. Lett. **29**, 382 (1972); D. J. Scalapino, Phys. Rev. Lett. **29**, 386 (1972).
[3]A. B. Migdal, Fermiony i bozony v sil'nykh polyakh (Fermions and Bosons in Strong Fields), Nauka, Moscow (1978); A. B. Migdal, Rev. Mod Phys. **50**, 107 (1978).
[4]A. B. Migdal, Phys. Rev. Lett. **31**, 257 (1973).
[5]A. B. Migdal, O. A. Markin, and I. N. Mishustin, Zh. Eksp. Teor. Fiz. **66**, 443 (1974) [Sov. Phys. JETP **39**, 212 (1974)].
[6]V. S. Butsev and D. Chultem, Phys. Lett. **B67**, 33 (1977).
[7]M. A. Troitskii, M. V. Koldaev, and N. I. Chekunaev, Pis'ma Zh. Eksp. Teor. Fiz. **25**, 136 (1977) [JETP Lett. **25**, 123 (1977)]; Zh. Eksp. Teor. Fiz. **46**, 662 (1977) [Sov. Phys. JETP **73**, 1258 (1977)].
[8]V. F. Dmitriev, Yad. Fiz. **24**, 913 (1976) [Sov. J. Nucl. Phys. **24**, 477 (1976)].
[9]A. B. Migdal, Phys. Lett. **52B**, 172 (1974); A. B. Migdal, Usp. Fiz. Nauk **123**, 369 (1977) [Sov. Phys. Usp. **20**, 879 (1977)]; A. B. Migdal *et al.*, Zh. Eksp. Teor. Fiz. **72**, 1247 (1977) [Sov. Phys. JETP **45**, 654 (1977)]; A. B. Migdal *et al.*, Phys. Lett. **B65**, 423 (1976).
[10]T. D. Lee and G. C. Wick, Phys. Rev. D **9**, 2291 (1974); T. D. Lee, Rev. Mod. Phys. **47**, 267 (1975).
[11]É. E. Sapershtein and M. A. Troitskii, Yad. Fiz. **22**, 257 (1975) [Sov. J. Nucl. Phys. **22**, 132 (1975)]; Izv. Akad. Nauk SSSR, Ser. Fiz. **40**, 95 (1976); Pis'ma Zh. Eksp. Teor. Fiz. **21**, 138 (1975) [JETP Lett. **21**, 62 (1975)].
[12]É. E. Sapershtein, S. V. Tolokonnikov, and S. A. Fayans, Izv. Akad. Nauk SSSR, Ser. Fiz. **41**, 1573 (1977).
[13]É. E. Sapershtein, S. V. Tolokonnikov, and S. A. Fayans, Izv. Akad. Nauk SSSR, Ser. Fiz. **41**, 2063 (1977).
[14]É. E. Sapershtein, S. V. Tolokonnikov, and S. A. Fayans, Pis'ma Zh. Eksp. Teor. Fiz. **25**, 548 (1977) [JETP Lett. **25**, 513 (1977)].
[15]M. Gyulassy and W. Greiner, Ann. Phys. (N.Y.) **109**, 485 (1977).
[16]M. Ericson and J. Delorme, Phys. Lett. **B76**, 182 (1978).
[17]J. Delorme, Phys. Lett. **B89**, 327 (1980).
[18]H. Toki and W. Weise, Phys. Rev. Lett. **42**, 1043 (1979).
[19]V. A. Khodel', Yad. Fiz. **19**, 792 (1974) [Sov. J. Nucl. Phys. **19**, 404 (1975)].
[20]É. E. Sapershtein, S. A. Fayans, and V. A. Khodel', Fiz. Elem. Chastits At. Yadra **9**, 221 (1978) [Sov. J. Part. Nucl. **9**, 91 (1978)].
[21]É. E. Sapershtein and V. A. Khodel', Yad. Fiz. **6**, 256 (1967) [Sov. J. Nucl. Phys. **6**, 186 (1967)].
[22]A. A. Carter *et al.*, Nucl. Phys. B26, 445 (1971).
[23]W. D. Myers and W. J. Swiatecki, Ann. Phys. (N.Y.) **55**, 395 (1969).
[24]G. E. Brown and W. Weise, Phys. Rep. C27, 1 (1976).
[25]H. Toki and W. Weise, Z. Phys. A292, 389 (1979).
[26]A. B. Migdal, Teoriya konechnykh fermi-sistem i svoĭstva atomnykh yader, Nauka, Moscow (1965); English translation: Theory of Finite Fermi Systems, Interscience, New York (1967).
[27]D. Pines and P. Nozières, The Theory of Quantum Liquids, Vol. 1, Benjamin, New York (1966).
[28]A. B. Migdal, N. A. Kirichenko, and G. A. Sorokin, Phys. Lett. **B50**, 411 (1974).

[29]É. E. Sapershteĭn, S. V. Tolokonnikov, and S. A. Fayans, Preprint No. 2571, I. V. Kurchatov Institute of Atomic Energy, Moscow (1975); Pis'ma Zh. Eksp. Teor. Fiz. 22, 529 (1975) [JETP Lett. 22, 258 (1975)]; Yad. Fiz. 25, 959 (1976) [Sov. J. Nucl. Phys. 25, 510 (1977)]; S. A. Fayans, E. E. Sapershteĭn, and S. V. Tolokonnikov, J. Phys. G 3, L51 (1977).
[30]V. A. Chepurnov, Yad. Fiz. 6, 955 (1967) [Sov. J. Nucl. Phys. 6, 696 (1967)].
[31]É. E. Sapershtein and V. A. Khodel', Yad. Fiz. 11, 760 (1970) [Sov. J. Nucl. Phys. 11, 425 (1970)].
[32]J. Meyer-ter-Vehn, Z. Phys. A287, 241 (1978).
[33]A. B. Migdal, Pis'ma Zh. Eksp. Teor. Fiz. 19, 539 (1974) [JETP Lett. 19, 284 (1974)].
[34]J. W. Negele, Phys. Rev. C 1, 1260 (1970).
[35]V. E. Starodubskiĭ, Yad. Fiz. 29, 884 (1979) [Sov. J. Nucl. Phys. 29, 454 (1979)].
[36]É. E. Sapershtein and V. E. Starodubskiĭ, Yad. Fiz. 30, 70 (1979) [Sov. J. Nucl. Phys. 30, 36 (1979)].
[37]H. J. Pirner, Phys. Lett. B67, 170 (1977).
[38]H. L. Anderson *et al.*, Phys. Rev. B 133, 392 (1964).
[39]E. Dey *et al.*, Helv. Phys. Acta 49, 778 (1976).
[40]J. Speth, Preprint, Jülich (1980).
[41]S. A. Fayans, E. E. Sapershteĭn, and S. V. Tolokonnikov, Nucl. Phys. A326, 463 (1979).
[42]V. M. Osadchiev and M. A. Troitskiĭ, Yad. Fiz. 6, 961 (1967) [Sov. J. Nucl. Phys. 6, 700 (1968)].
[43]É. E. Sapershtein and S. V. Tolokonnikov, Izv. Akad. Nauk SSSR, Ser. Fiz. 42, 1980 (1978).
[44]S. Barshay and G. E. Brown, Phys. Lett. B47, 107 (1973).
[45]J. Meyer-ter-Vehn, in: Proc. Intern. Conf. on High Energy Physics and Nuclear Structure, Zürich (1977), p. 127.
[46]A. Heusler and P. von Brentano, Ann. Phys. (N.Y.) 75, 381 (1973).
[47]A. B. Migdal, Zh. Eksp. Teor. Fiz. 46, 1680 (1964) [Sov. Phys. JETP 19, 1136 (1964)].
[48]G. A. Pik-Pichak, Yad. Fiz. 6, 265 (1967) [Sov. J. Nucl. Phys. 6, 192 (1968)].
[49]R. Bauer *et al.*, Nucl. Phys. A209, 535 (1973).
[50]J. Speth, E. Werner, and W. Wild, Phys. Rep. C33, 1 (1977).
[51]V. A. Sadovnikova, Yad. Fiz. 32, 1527 (1980) [Sov. J. Nucl. Phys. 32, 791 (1980)].
[52]J. Hamamoto, Phys. Lett. B61, 343 (1976).
[53]L. D. Landau and E. M. Lifshits, Élektrodinamika sploshnykh sred, Nauka Moscow (1960); English translation: Electrodynamics of Continuous Media, Pergamon Press, Oxford (1960).
[54]W. M. Alberico, M. Ericson, and A. Molinari, Phys. Lett. B92, 153 (1980).
[55]H. Toki and W. Weise, Z. Phys. A295, 187 (1980).
[56]S. A. Fayans, E. E. Sapershteĭn, and S. V. Tolokonnikov, Preprint IAE-3254, Moscow (1980); Phys. Lett. B92, 33 (1980).
[57]W. T. Wagner *et al.*, Phys. Rev. C 12, 757 (1975).
[58]W. T. H. Van Oers *et al.*, Phys. Rev. C 10, 307 (1974).
[59]F. D. Becchetti, Jr. and G. W. Greenlees, Phys. Rev. 182, 1190 (1969).
[60]B. M. Golovin and A. M. Rozanova, Preprint R-2861 [in Russian], JINR, Dubna (1966).
[61]Indiana University Cyclotron Facility Annual Report (1979), p. 138.
[62]G. T. Emery, Report on 1980 RCNP Intern. Symposium on Highly Excited States in Nuclear Reactions, May 12–16, Osaka, Japan (1980).
[63]H. Toki and W. Weise, Phys. Lett. B92, 265 (1980).
[64]M. Haji-Saeid *et al.*, Preprint RU80-212, USA (1980).
[65]R. S. Henderson *et al.*, Indiana University Cyclotron Facility Annual Report (1979), p. 1.
[66]R. E. Segel *et al.*, *ibid.*, p. 4.
[67]A. M. Dyagaev, Pis'ma Zh. Eksp. Teor. Fiz. 22, 181 (1975) [JETP Lett. 22, 83 (1975)].
[68]H. Sagawa *et al.*, Nucl. Phys. A322, 361 (1979).
[69]J. Dubach and W. C. Haxton, Phys. Rev. Lett. 41, 1453 (1978).
[70]J. Heisenberg, Lect. Notes Phys. 108, 33 (1979).
[71]J. Lichtenstadt *et al.*, Phys. Rev. C 20, 497 (1980).

Translated by Julian B. Barbour